J Physiol 587.10 (2009) pp 2233–2253

The Journal of Physiology

Functional K_{ATP} channels in the rat retinal microvasculature: topographical distribution, redox regulation, spermine modulation and diabetic alteration

Eisuke Ishizaki[1], Masanori Fukumoto[1] and Donald G. Puro[1,2]

[1]*Department of Ophthalmology & Visual Sciences and* [2]*Department of Molecular & Integrative Physiology, University of Michigan, Ann Arbor, MI 48105, USA*

The essential task of the circulatory system is to match blood flow to local metabolic demand. However, much remains to be learned about this process. To better understand how local perfusion is regulated, we focused on the functional organization of the retinal microvasculature, which is particularly well adapted for the local control of perfusion. Here, we assessed the distribution and regulation of functional K_{ATP} channels whose activation mediates the hyperpolarization induced by adenosine. Using microvascular complexes freshly isolated from the rat retina, we found a topographical heterogeneity in the distribution of functional K_{ATP} channels; capillaries generate most of the K_{ATP} current. The initiation of K_{ATP}-induced responses in the capillaries supports the concept that the regulation of retinal perfusion is highly decentralized. Additional study revealed that microvascular K_{ATP} channels are redox sensitive, with oxidants increasing their activity. Furthermore, the oxidant-mediated activation of these channels is driven by the polyamine spermine, whose catabolism produces oxidants. In addition, our observation that spermine-dependent oxidation occurs predominately in the capillaries accounts for why they generate most of the K_{ATP} current detected in retinal microvascular complexes. Here, we also analysed retinal microvessels of streptozotocin-injected rats. We found that soon after the onset of diabetes, an increase in spermine-dependent oxidation at proximal microvascular sites boosts their K_{ATP} current and thereby virtually eliminates the topographical heterogeneity of functional K_{ATP} channels. We conclude that spermine-dependent oxidation is a previously unrecognized mechanism by which this polyamine modulates ion channels; in addition to a physiological role, spermine-dependent oxidation may also contribute to microvascular dysfunction in the diabetic retina.

(Received 11 January 2009; accepted after revision 12 March 2009; first published online 16 March 2009)

Corresponding author D. G. Puro: Department of Ophthalmology and Visual Sciences, University of Michigan, 1000 Wall Street, Ann Arbor, MI 48105, USA. Email: dgpuro@umich.edu

Abbreviations Carboxy-H_2DCFDA, 6-carboxy-2′,7′-dichlorodihydrofluorescein diacetate; DCF, dichlorofluorescein; DFMO, DL-α-difluoromethylornithine; DMSO, dimethyl sulfoxide; DTNB, 5,5′-dithiobis(2-nitrobenzoic acid); DTT, dithiothreitol; MDG, *N*-methyl-D-glucamine; ROI, regions of interest.

As with nearly all tissues, the function of the retina is dependent upon the circulatory system. Yet, unlike nearly all other vascular beds, the blood supply of the retina must meet the special requirement of providing substrates to a tissue whose translucency is essential for its function. During most of evolution, this challenge was met by having the retina rely exclusively upon the diffusion of oxygen and nutrients from the underlying choriocapillaris; retinas lacked intrinsic blood vessels, which could interfere with light passing to the photoreceptors. In contrast, the retinas of most mammals and all primates are vascularized. This is thought to provide a physiological advantage because retinal thickness is not limited by the need for energy substrates to diffuse from an extrinsic source (Chase, 1982). As a consequence, the inner synaptic layer of the vascularized retina is significantly enlarged (Buttery *et al.* 1991) and presumably performs more complex information processing. On the other hand, a disadvantage of retinal blood vessels is that they can block photons. As an apparent adaptation to minimize this threat to vision,

E. Ishizaki and M. Fukumoto contributed equally to this work. This paper has online supplemental material.

© 2009 The Authors. Journal compilation © 2009 The Physiological Society

DOI: 10.1113/jphysiol.2009.169003

the density of retinal capillaries is particularly low (Funk, 1997). However, the relative paucity of capillaries leaves little functional reserve.

How is the retina's circulatory system adapted so that its low density of capillaries effectively meets the stringent metabolic needs of neurons? One crucial adaptation that helps meet this challenge is the independence of the retinal vasculature from extrinsic inputs. While blood flow in most tissues is subject to CNS oversight via autonomic pathways, the blood vessels of the retina lack automonic innervation (Ye *et al.* 1990). Furthermore, a tight blood–retina barrier prevents circulating vasoactive molecules from directly affecting the contractile tone of abluminal mural cells. Thus, the circulatory system of the retina functions quite independently, and retinal blood flow is not compromised due to the metabolic demands of other tissues.

Another important adaptation of the circulatory system of the retina is the decentralization of control. Supporting this concept, evidence is accumulating that the mural cells of the capillaries, i.e. the pericytes, are poised to play an active role in the regulation of retinal blood flow. Consistent with this role, it has long been established that these cells express contractile proteins (Shepro & Morel, 1993) and can contract and relax in response to a variety of vasoactive signals (Puro, 2007). More recently, Peppiatt and her colleagues elegantly demonstrated that a change in the contractile tone of pericytes causes vasodilatation and vasoconstriction of capillaries within the intact retina (Peppiatt *et al.* 2006). Suggestive that this decentralized control of local perfusion is particularly important in the retina, its capillaries have a higher density of pericytes than the microvasculature of any other tissue (Shepro & Morel, 1993).

Also consistent with pericyte-containing microvessels being functionally organized to play a role in blood flow regulation, a retinal capillary network plus the feeder vessel linking it with a myocyte-encircled arteriole constitute an interactive multicellular complex in which efficient electrotonic transmission is mediated via gap junction pathways (Wu *et al.* 2006). Peppiatt and colleagues have provided additional functional evidence for this interactive organization by showing in the intact retina that a localized electrical stimulation of a pericyte not only increases the contractile tone of the stimulated pericyte, but also evokes contractions in distant mural cells (Peppiatt *et al.* 2006). However, despite recent progress, much remains to be elucidated about the functional organization of the feeder vessel–capillary complex within the retinal microvasculature.

To help clarify how the retinal microvasculature is functionally organized, this study focused on the distribution and regulation of functional K_{ATP} channels in microvascular complexes freshly isolated from the adult rat retina. These ion channels are of interest because they mediate the hyperpolarizing response of the retinal vasculature to the vasoactive signals, adenosine and dopamine (Li & Puro, 2001; Wu *et al.* 2001). Here, we report that there is a topographical heterogeneity in the distribution of functional K_{ATP} channels; most of the K_{ATP} current is generated in the capillaries. We also observed that microvascular K_{ATP} channels are redox sensitive with oxidants markedly increasing their activity. In addition, we discovered that the activity of these channels in retinal microvessels is driven by the polyamine spermine, whose catabolism produces hydrogen peroxide and other potent oxidants (Wang & Casero, 2006). Furthermore, we found that spermine-dependent oxidation normally occurs predominately in the capillaries. Our experiments indicate that this localization of spermine-dependent oxidation accounts for why most of the functional K_{ATP} channels of the retinal microvasculature are in the capillaries.

In this study, we also analysed the location and regulation of K_{ATP} currents in retinal microvascular complexes of rats made diabetic by streptozotocin. Identifying functional changes in the microvasculature of the diabetic retina is important because blood flow dysregulation occurs early in the course of diabetes (Kohner *et al.* 1995) and may play a role in the progression of diabetic retinopathy, which is an important sight-threatening disorder. Here, we report that a diabetes-induced increase in spermine-dependent oxidation within the feeder vessels results in a fundamental alteration in the functional organization of the retinal microvasculature. Namely, the topographical heterogeneity of functional K_{ATP} channels becomes minimized soon after the onset of diabetes. Thus, our study indicates that spermine-dependent oxidation is likely to have a pathophysiological, as well as the physiological, role in the retinal microvasculature.

Methods

Animal use conformed to the guidelines of the Association for Research in Vision and Ophthalmology and was approved by the University of Michigan Committee on the Use and Care of Animals. This study used 103 Long–Evans rats (Charles River, Cambridge, MA, USA), which were maintained on a 12 h alternating light–dark cycle and received food and water *ad libitum*.

Experimental model of diabetes

Diabetes was induced by an intraperitoneal injection of streptozotocin (150 mg kg^{-1} diluted in 0.8 ml citrate buffer) into 5-week-old Long–Evans rats that had fasted for 5 h. In this study, we used 23 rats made hyperglycaemic for 6.1 ± 0.4 weeks; immediately before harvesting the

© 2009 The Authors. Journal compilation © 2009 The Physiological Society

retinal microvessels from diabetic rats, the blood glucose level was 317 ± 9 mg dl^{-1}.

Microvessel isolation

Using our previously described tissue print procedure (Kobayashi & Puro, 2007), we isolated complexes of microvessels from the retinas of adult non-diabetic and diabetic rats. With a rising concentration of carbon dioxide, 6- to 14-week-old non-diabetic and diabetic rats were killed. Retinas were rapidly removed and placed in solution A, which consisted of 140 mM NaCl, 3 mM KCl, 1.8 mM $CaCl_2$, 0.8 mM $MgCl_2$, 10 mM Na-Hepes, 15 mM mannitol and 5 mM glucose at pH 7.4 with osmolarity adjusted to 310 mosmol l^{-1}, as measured by a vapour pressure osmometer (Wescor, Inc., Logan, UT, USA). After adherent vitreous was carefully removed with fine forceps, each retina was cut into quadrants and incubated for 22–26 min at 30°C in 2.5 ml Earle's balanced salt solution that was supplemented with 0.5 mM EDTA, 6 U papain (Worthington Biochemicals, Freehold, NJ, USA) and 2 mM cysteine; the pH was adjusted to approximately 7.4 by bubbling 5% carbon dioxide. For each new lot of papain, the duration of incubation was empirically adjusted to optimize the yield of microvascular complexes. After incubation in the papain-containing solution, the pieces of retina were transferred to a 60 mm Petri dish containing 5 ml of solution A. Then, one by one, each retinal quadrant was positioned with its vitreal surface up in a glass-bottomed chamber, which contained 1 ml of solution A. Subsequently, each retinal quadrant was sandwiched between the bottom of the chamber and a 15 mm diameter glass coverslip (Warner Instrument Corp., Hamden, CT, USA) that was gently applied onto the vitreal surface of the retina. After approximately 30 s of compression, the coverslip was carefully removed; it contained adherent complexes of retinal microvessels. All experiments were performed at room temperature, i.e. 22–23°C. Unless otherwise noted, microvessels were used within 4 h of isolation from the retina.

Each microvascular complex used in this study included, from proximal to distal, (1) an arteriole encircled by 'doughnut-shaped' myocytes, (2) a bifurcating feeder vessel with ≥ 5 'dome-shaped' mural cell somas per 100 μm, and (3) a capillary network whose abluminal mural cells, the pericytes, appear as 'bumps on a log' and have a density of ≤ 4 per 100 μm. Of note, in 49 of 50 successively isolated microvascular complexes used in the course of the study presented here, a feeder vessel branched once before reaching the capillary network; this branch point was 238 ± 78 μm distal to the myocyte-encircled arteriole and 184 ± 26 μm proximal to the capillaries. A photomicrograph illustrating these morphological features and a discourse concerning the anatomy of retinal microvascular complexes freshly isolated from the rat retina are in a recent publication (Matsushita & Puro, 2006); additional photomicrographs of retinal microvessels isolated by our technique, as well as time-lapse movies showing vasomotor responses of isolated retinal microvessels to a variety of vasoactive signals, are available (Kawamura *et al.* 2003; Wu *et al.* 2003; Kawamura *et al.* 2004; Yamanishi *et al.* 2006; Puro, 2007).

Electrophysiology

A microvessel-containing coverslip was positioned in a recording chamber (volume = 1 ml), which was perfused ($\sim$1.5 ml min^{-1}) with solutions from a gravity-fed system using multiple reservoirs. The recording chamber and the reservoirs for the perfusates were open to the air; no additional oxygenation was administered. In most experiments, solution A (see above for its ingredients) was used as the perfusate, although in some experiments the perfusate was solution B, which contained 97.5 mM KCl, as well as 43 mM NaCl, 1.8 mM $CaCl_2$, 0.8 mM $MgCl_2$, 10 mM Na-Hepes, 15 mM mannitol and 5 mM glucose, with the pH at 7.4 and the osmolarity adjusted to 310 mosmol l^{-1}. Pipettes for perforated-patch recordings were filled with a solution consisting of 50 mM KCl, 65 mM K_2SO_4, 6 mM $MgCl_2$, 10 mM K-Hepes, 60 μg ml^{-1} amphotericin B and 60 μg ml^{-1} nystatin at pH 7.4 with the osmolarity adjusted to 280 mosmol l^{-1}. A recording pipette having a resistance of 5–10 MΩ was mounted in the holder of a patch-clamp amplifier (Axopatch 200B, MDS Analytical Technologies, Union City, CA, USA; Dagan 3900, Dagan Corp., Minneapolis, MN, USA), which was used in the voltage-clamp or current-clamp mode. Positioning the tip of a recording pipette onto a microvascular mural cell was controlled with a piezoelectric-based micromanipulator (Exfo, Mississauga, Ontario, Canada) while the microvessel of interest was viewed at ×400 magnification with phase-contrast optics. As suction was applied to the back end of the pipette, a ≥ 10 GΩ seal formed. We used recordings in which the access resistance became less than 25 MΩ within 5 min after gigaohm seal formation. Throughout each recording, the access resistance was monitored, and if there was a significant change, the recording was terminated.

Currents and voltages were filtered with a four-pole Bessel filter, digitally sampled using a DigiData 1200B or 1440A acquisition system (MDS Analytical Technologies) and stored by a computer equipped with pCLAMP (version 8.2 or 10, MDS Analytical Technologies) and Origin (v. 7, OriginLab Corp., Northampton, MA, USA) software for data analysis and graphics display. For the generation of current–voltage (I–V) plots, currents were evoked by protocols that were controlled by pCLAMP

© 2009 The Authors. Journal compilation © 2009 The Physiological Society

and consisted of either steps of voltage or negative to positive ramping (50 mV s^{-1}) of voltage. Adjustment for the calculated liquid junction potential (Barry, 1994) was made after data collection. The membrane potentials used in the experiments presented in Figs 1, 3*A* and 11*A* and *B* were from current-clamp recordings. For the experiments presented in Fig. 7, the zero-current potential was defined as the membrane potential.

For comparison of pinacidil-induced currents, mean conductances calculated at 10 mV intervals, from −98 mV to −38 mV for assays done in solution A and from −10 mV to +20 mV for assays performed in solution B, were compared using Student's paired *t*-test. As discussed previously (Matsushita & Puro, 2006), the currents detected by a perforated-patch pipette sealed onto a mural cell include not only those generated in the abluminal cell, but also currents transmitted electronically via gap junction pathways (Oku *et al.* 2001; Wu *et al.* 2006) from many neighbouring endothelial and mural cells. Determination of membrane capacitance by the method of Zhao & Santos-Sacchi (1998) did not reveal a significant ($P > 0.2$) difference in the membrane capacitance calculated from recordings made at sites on feeder vessels compared with those made on capillaries in solution A. Also, the membrane capacitances calculated from recordings made at sites on feeder vessels and capillaries were not significantly affected ($P > 0.2$) by spermine (5 mM), 5,5′-dithiobis(2-nitrobenzoic acid) (DTNB, 500 μM), or dithiothreitol (DTT, 3 mM), or by diabetes. However, as we have reported (Matsushita & Puro, 2006), solution B, which contains 97.5 mM K^+, decreased the membrane capacitance by approximately 4-fold ($P < 0.001$), as compared with solution A (3 mM K^+).

Upon completion of an electrophysiological recording, a photomicrograph of the sampled microvascular complex was obtained. This permitted subsequent independent determination of the recording pipette's location within the microvascular complex, e.g. capillary, feeder vessel or myocyte-encircled arteriole.

Miniperfusion

In a number of experiments voltage was monitored via a perforated-patch pipette as pinacidil was miniperfused onto various microvascular sites via pipettes that were

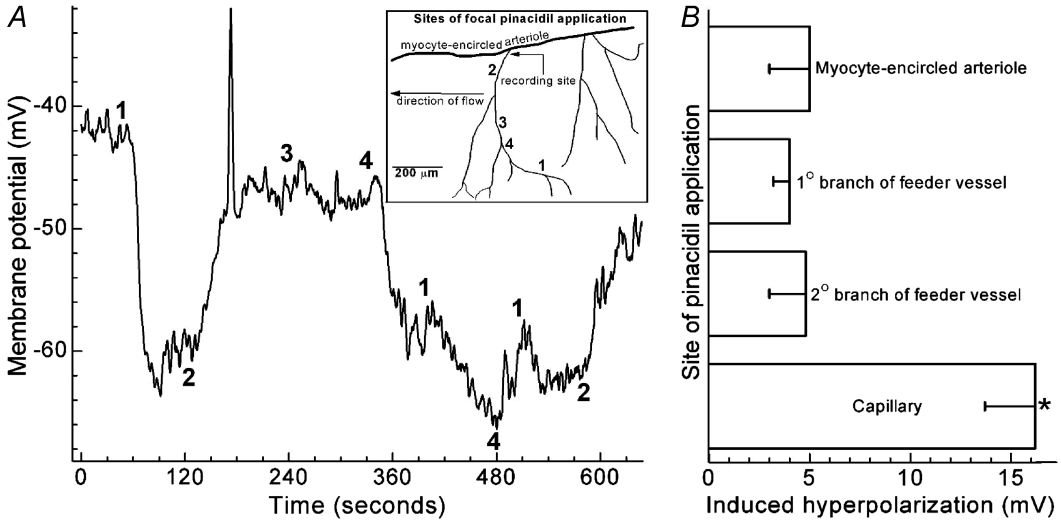

Figure 1. Use of focal application of the K_{ATP} activator pinacidil to map the distribution of functional K_{ATP} channels within the retinal microvasculature
A, effect on the membrane potential of miniperfusing pinacidil at various microvascular sites. Continuous record of the membrane potential monitored via a perforated-patch pipette sealed onto a mural cell located on a freshly isolated microvascular complex. Pinacidil was focally applied at various sites on a microvessel extending from a myocyte-encircled arteriole. The numbers located adjacent to the voltage trace indicate the time at which the tip of the pinacidil-containing micropipette was moved to the microvascular site shown in the drawing (inset). Pinacidil application at the more distal microvascular sites, i.e. 1 and 4, induced greater hyperpolarizations than its application at the more proximal locations. At ∼180 s on this voltage record, there was an action potential, a relatively common depolarization-induced phenomenon. *B*, microvascular site of pinacidil application *versus* the amplitude of the pinacidil-induced hyperpolarization. Data are from 19 experiments similar to the one illustrated in *A*. Pinacidil was miniperfused onto myocyte-encircled arterioles ($n = 6$), primary branches of feeder vessels ($n = 18$), secondary feeder vessel branches ($n = 11$) and capillaries ($n = 17$). For the myocyte-encircled arteriole group, recordings were from the arteriole; for the other groups, recordings were from mural cells on the primary feeder vessel branch. *$P \leq 0.0047$ for the difference in the hyperpolarization induced by applying pinacidil onto capillaries as compared with application at the more proximal locations.

© 2009 The Authors. Journal compilation © 2009 The Physiological Society

identical in shape to the recording pipettes, were filled with solution A supplemented with the K_{ATP} activator pinacidil (1 mM from a 100 mM stock in DMSO), and were mounted on a micromanipulator (Exfo); pressure ejection was not used. In the miniperfusion experiments, the concentration of pinacidil that reached the surface of a sampled microvessel was unknown, although substantial dilution certainly occurred as the small volume leaking from the micropipette entered the bathing solution and then briskly flowed through the recording chamber. In control experiments ($n = 5$) in which the recording chamber was perfused with solution A, the miniperfusion of solution A supplemented with 1% DMSO did not cause a detectable change in the membrane potential of retinal microvessels.

In other miniperfusion experiments, pipettes were filled with solution C, which contained 3 mM KCl, as well as 43 mM NaCl, 1.8 mM $CaCl_2$, 0.8 mM $MgCl_2$, 10 mM Na-Hepes, 15 mM mannitol, 94.5 mM *N*-methyl-D-glucamine (NMDG)-Cl and 5 mM glucose with the pH at 7.4 and the osmolarity adjusted to 310 mosmol l^{-1}. As voltage was monitored via a perforated-patch pipette, solution C was miniperfused systematically at sites along a microvessel bathed in solution B, which was identical to solution C except for having 97.5 mM KCl and no NMDG-Cl. For the plot in Fig. 3*A*, the magnitude of the hyperpolarization evoked by miniperfusion of solution C at the site of the recording pipette was used to normalize the voltage changes detected when solution C was applied at other microvascular sites.

During a miniperfusion experiment, each location of the miniperfusion pipette was carefully noted on a drawing of the microvascular complex, and in nearly all cases, the sites were also photographically documented in a photomicrograph.

Microvessel transection

In certain experiments, a micropipette was used to transect a microvascular complex. The micropipettes used for this task were identical in shape to the recording pipettes. The position of the micropipette tip was controlled by a piezoelectric-based micromanipulator (Exfo) as it was viewed at ×400 magnification with an inverted microscope equipped with phase-contrast optics. Transection was at the feeder vessel–capillary junction when only one of the pair of secondary branches of a feeder vessel connected to a capillary network; in other cases, transection was at the junction of the primary and secondary feeder vessel bifurcation. Although a transient depolarization often occurred as a microvessel was transected, the resting membrane potential recorded $\geq$ 5 min after transection was not significantly different ($P = 0.4$, paired *t*-test) from the pre-transection voltage monitored at feeder vessel ($n = 3$) and capillary ($n = 4$) sites. In addition, membrane capacitances calculated from perforated-patch recordings of feeder vessels ($n = 22$) and capillary ($n = 25$) after microvessel transection were not significantly ($P > 0.2$) different.

Imaging of intracellular oxidants

Freshly isolated retinal microvascular complexes were exposed to 10 μM 6-carboxy-2′, 7′-dichlorodihydrofluorescein diacetate (carboxy-H_2DCFDA; Invitrogen, Eugene, OR, USA) in solution A at 30°C for 60–90 min. The microvessels were then bathed in solution A (without the dye) for 30–90 min in order to allow time for the dye to be cleaved by intracellular esterases to form carboxy-H_2DCF, which upon oxidation becomes fluorescent dichlorofluorescein (DCF). Subsequently, a microvessel-containing coverslip was positioned in a 200 μl recording chamber, which was perfused ($\sim$1.5 ml min^{-1}) via a gravity-fed system using multiple reservoirs. Microvessels were observed using a Nikon Eclipse TE300 microscope at ×400 using a ×40 water-immersion objective. Digital imaging of DCF fluorescence was performed at room temperature using an optical sensor (Sensicam, Cooke Corp., Auburn Hills, MI, USA). The light source was a high intensity mercury lamp coupled to an Optoscan Monochromator (Cairn Research Ltd, Faversham, UK). Fluorescence was detected with excitation and emission wavelengths of 490 and 520 nm, respectively. Control of the imaging equipment and the collection of data were facilitated by the Axon Imaging Workbench software (MDS Analytical Technologies). To minimize photooxidation, illumination was limited to 400 ms exposures at 30–90 s intervals. Autofluroescence was not detected in microvessels that had not been exposed to carboxy-H_2DCFDA. In microvascular complexes exposed to carboxy-H_2DCFDA, both mural cells and endothelial cells became loaded with this dye. No attempt was made to selectively detect fluorescence in mural or endothelial cells; fluorescence from both cell types was detected.

Regions of interest (ROIs) were selected on microvessels and in order to determine background fluorescence, also on cell-free areas of the coverslip. Subtraction of the background fluorescence from the intensity of fluorescence measured in microvascular ROIs yielded the net microvascular fluorescence. For each group of ROIs, the average net fluorescence during the 300 s prior to the onset of spermine or hydrogen peroxide exposure was used as the control value. Subsequent net fluorescence measurements were plotted in Fig. 8 as the percentage of the control value.

© 2009 The Authors. Journal compilation © 2009 The Physiological Society

Chemicals. Unless otherwise noted, chemicals were obtained from Sigma (St Louis, MO, USA). For the bath application of pinacidil, a 5 mM stock in DMSO was diluted 1000-fold in the bathing solution; 0.1% DMSO does not have a detectable effect on retinal microvascular currents.

Statistics and data analysis. Data are given as means ± S.E.M. Unless noted otherwise, probability was evaluated by Student's two-tailed *t*-test. In Fig. 3*A*, Origin software was used to fit a first-order exponential decay.

Results

Topographical distribution of functional K_{ATP} channels

To better characterize the functional organization of the retinal microvasculature, we assessed the topographical distribution of functional K_{ATP} channels, which are of interest because they mediate the hyperpolarizing effect of the vasoactive signals adenosine and dopamine (Li & Puro, 2001; Wu *et al.* 2001). To determine where K_{ATP} currents are generated within the retinal microvasculature, we employed several experimental strategies each of which involved the use of microvascular complexes freshly isolated from the adult rat retina. For each experiment strategy, ionic currents or voltage changes induced by the selective K_{ATP} channel activator pinacidil were monitored via a perforated-patch pipette sealed onto a mural cell located on the feeder vessel (proximal) portion or the capillary portion of an isolated microvascular complex.

An experimental advantage of using isolated microvessels is that mural cells can be unambiguously seen and patched onto. As illustrated in a previous study (Matsushita & Puro, 2006), a capillary's mural cells, i.e. the pericytes, were identified by the distinctive 'bump on a log' appearance of their somas, which are at a density of ≤ 4 somas per 100 μm; in our preparations of isolated retinal microvessels, pericytes are reliably distinguished from the long and thin endothelial cells that form the capillary tube. Our earlier publications show images of single pericytes loaded with a dye administered via a patch pipette (Fig. 1*B* and *C* in Oku *et al.* 2001 and Fig. 6*B* of Kawamura *et al.* 2002); in the course of these studies, never (0 of 32) was an endothelial cell directly filled with dye when the goal was to patch onto a pericyte (T. Kodama, H. Oku & D. Puro, unpublished observations). In isolated microvascular complexes, it is also straightforward to identify the mural cells of feeder vessels, which are the vessels linking smooth muscle-encircled arterioles with capillaries. These mural cells are dome shaped, as illustrated in Matsushita & Puro (2006), and have been characterized as atypical smooth muscle cells (Ikebe *et al.* 2001). Because the mural cells of the feeder vessels are closely packed together, i.e. ≥ 5 somas per 100 μm (Matsushita & Puro, 2006), and cover most of the endothelial surface, they can be reliably sealed onto by a patch pipette.

An important consequence of the highly efficient gap junction-mediated electrotonic transmission within retinal microvessels (Wu *et al.* 2006) is that perforated-patch recordings from mural cells located on feeder vessels and capillaries detect currents and voltages that are generated, not only by the sampled cell, but also by numerous other microvascular cells (Matsushita & Puro, 2006). In fact, our studies indicate that when a microvessel is bathed in solution A (our standard 3 mM K^+ solution), approximately 95% of the current detected via a perforated-patch pipette sealed onto a mural cell is generated by other cells located throughout the microvascular complex (Matsushita & Puro, 2006). Thus, K_{ATP} channels in mural cells and endothelial cells can contribute to the current detected in this perforated-patch study. Here, our aim was not to assess the relative contributions of mural and endothelial cells to the K_{ATP} conductance, but to determine the relative roles of the feeder vessels and the capillaries in the generation of hyperpolarizing K_{ATP} currents.

The first experimental strategy that we used to help characterize the location within the retinal microvasculature of functional K_{ATP} channels was to focally apply pinacidil at various sites along a microvessel while a perforated-patch pipette sealed onto a mural cell monitored voltage. For these experiments in which the bathing solution was solution A, the microvascular location of the recording pipette was not critical because as we reported previously (Wu *et al.* 2006), a locally generated voltage change spreads throughout a feeder vessel–capillary complex with minimal attenuation, i.e. ~2% decay per 100 μm. Our experiments using the miniperfusion of pinacidil, revealed that the size of the pinacidil-induced hyperpolarization varied markedly depending on the microvascular site at which the K_{ATP} activator was applied. Figure 1*A* illustrates a typical experiment. When pinacidil was applied onto the capillary portion of the microvascular complex (site 1), the membrane potential increased from −42 to −62 mV. However, when the pinacidil-filled pipette was subsequently moved to the primary branch of the feeder vessel (site 2), the membrane potential decreased towards the resting value. Application of pinacidil onto a secondary branch of this feeder vessel (site 3) also had a minimal effect. On the other hand, when the miniperfusion pipette was positioned near the feeder vessel–capillary junction (site 4), the membrane potential increased. Return of the miniperfusion pipette to site 1 resulted in further hyperpolarization. In 19 similar experiments in which perforated-patch recordings were made at sites on the primary branch of feeder vessels, we confirmed that the miniperfusion of pinacidil onto capillaries, as compared to

© 2009 The Authors. Journal compilation © 2009 The Physiological Society

proximal microvascular sites, induced significantly greater ($P = 0.0017$) hyperpolarizations (Fig. 1*B*). Thus, results of experiments using the focal application of pinacidil were consistent with functional K_{ATP} channels being particularly plentiful in the capillary network, as compared with the feeder vessels, of the retinal microvasculature.

In addition to assessing the effect on voltage of focally applying pinacidil, we used other experimental strategies to test the hypothesis that functional K_{ATP} channels are predominately located in the capillaries. A potential pitfall with miniperfusion is that diffusion of pinacidil to distant microvascular sites may result in misleading conclusions. Also, we wished to exclude the potentially confounding effect of membrane resistance on the magnitude of an induced voltage change. For these reasons, we performed a series of experiments in which the effect of pinacidil on ionic currents was assessed.

To facilitate comparison of the pinacidil-induced currents generated in feeder vessels and capillaries, microvascular complexes were transected at their feeder vessel–capillary junctions. This technique permitted an independent assessment of the response of feeder vessels and capillaries to pinacidil. Results of one such experiment are shown in Fig. 2*A–D* in which the sketch in panel *A* shows the locations of the perforated-patch recordings, as well as the site of transection. Shown in Fig. 2*B* are the current–voltage (*I–V*) relations recorded via a perforated-patch pipette sealed onto a mural cell in the feeder vessel portion of the microvascular complex *prior* to transection. Initially, an *I–V* plot was generated when the recording chamber was perfused with solution A without any additives (squares). Then, 5 μM pinacidil was added to solution A (circles). Consistent with the activation of K_{ATP} channels, pinacidil induced a hyperpolarizing current that had a reversal potential near the equilibrium potential for K^+ (E_K), i.e. −103 mV. After transection of this microvessel at its feeder vessel–capillary junction, the *I–V* relations recorded at the feeder vessel site no longer showed a significant ($P = 0.8$) pinacidil-induced current (Fig. 2*C*). In contrast, when a perforated-patch recording was subsequently obtained from the capillary portion of this transected microvessel (site D in the sketch), pinacidil induced a robust hyperpolarizing current whose reversal potential was near E_K (Fig. 2*D*). Thus, in the microvessel studied in Fig. 2*A–D*, nearly all of the pinacidil-induced current was generated in the capillary portion. As shown in Fig. 2*E* and *F*, a series of additional experiments using transected microvessels confirmed that capillaries generated a significantly greater ($P = 0.0003$) pinacidil-induced current than did the feeder vessels.

Also consistent with functional K_{ATP} channels being located chiefly in the capillaries, we observed that the membrane potential recorded in the capillary network of a transected microvascular complex increased from -36 ± 2 mV to -67 ± 5 mV ($n = 12$) during exposure to 5 μM pinacidil. In contrast, in the feeder vessel portion of a transected microvessel, pinacidil induced a significantly smaller ($P = 0.004$) voltage change, from -38 ± 2 to -43 ± 2 mV ($n = 9$). Thus, the results of the experiments using transected microvessels were consistent with the observations made in our miniperfusion experiments (Fig. 1). We concluded that these two experimental strategies, i.e. transected microvessels and pinacidil miniperfusion, provided strong evidence supporting the idea that most of the pinacidil-induced hyperpolarizing current detected in retinal microvascular complexes is generated in the capillary network.

To complement results obtained with the use of focal pinacidil application and microvessel transection, we employed a third experimental strategy for comparing the pinacidil-induced conductances of feeder vessels and capillaries. We took advantage of an earlier observation (Matsushita & Puro, 2006) that a high extracellular K^+ solution (solution B) markedly decreases the membrane capacitance. If, as seems likely, this decrease in capacitance reflects a decrease in the efficacy of electrotonic transmission, then use of solution B would help us identify where within a microvascular complex K_{ATP} currents are generated. To confirm this experimental strategy, we first assessed the rate at which voltage decays as it spreads along a microvessel. As shown in Fig. 3*A*, the amplitude of an induced hyperpolarization decayed by ∼33% over a distance of 100 μm and by ∼90% at a distance of 400 μm. Thus, when solution B is used, nearly all of the current detected via a perforated-patch pipette is generated within ∼400 μm of the recording site. This contrasts with our earlier report that in solution A, a locally generated hyperpolarization spreads throughout much of a microvascular complex because it decays by only 2% per 100 μm (Wu *et al.* 2006). Based on our observations that there is an ∼90% decay per 400 μm in microvessels bathed in solution B and that the feeder vessel portion (primary branch plus a secondary branch) is 422 ± 26 μm in length ($n = 50$ successively isolated retinal microvascular complexes), it appears that in solution B a recording made at a proximal site on a feeder vessel detects current that is almost exclusively generated within the feeder vessel portion of the microvascular complex. Conversely, recording from sites > 400 μm distal to the feeder vessel–capillary junction detects currents generated predominately in the capillaries.

Recordings made at feeder vessel and capillary sites in microvessels bathed in solution B are illustrated in Fig. 3*B–D*. Figure 3*B* shows that the effect of pinacidil on the *I–V* relations was minimal when the recording pipette was sealed onto a mural cell located on a feeder vessel. However, in a recording from the capillary portion of the same microvascular complex, pinacidil reversibly increased the current (Fig. 3*C*). A series of experiments confirmed that the pinacidil-induced

© 2009 The Authors. Journal compilation © 2009 The Physiological Society

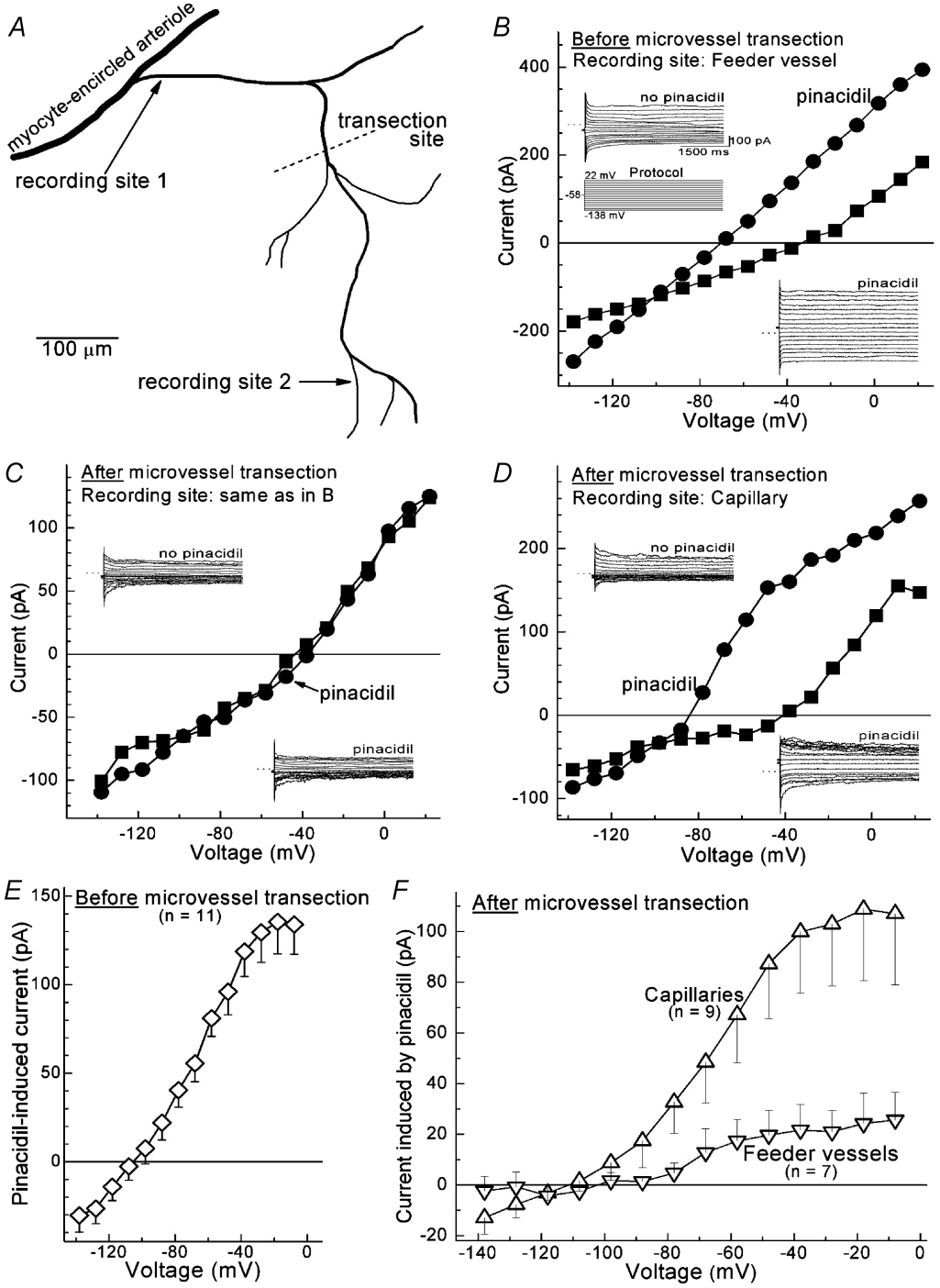

Figure 2. Use of transected microvessels to compare pinacidil-induced currents generated in feeder vessels and capillaries

A, sketch of the freshly isolated microvascular complex studied in panels *B–D*. Arrows point to the location of the perforated-patch recordings made before (site 1) and after transection of the microvessel (site 2). *B*, *I–V* relations recorded via a perforated-patch pipette sealed onto a mural cell located on the feeder vessel portion (site 1 in panel *A*) of the *intact* microvascular complex. The recording chamber was perfused with solution A without (squares) and with (circles) 5 μM pinacidil. Insets show the current traces used to generate *I–V* plots. The scales for current and time, as well as the stimulus protocol, apply for all current traces in this figure. Dotted lines adjacent to the current traces indicate the zero-current level. *C*, *I–V* relations recorded at the same proximal site as in panel *B*, but after the microvessel had been *transected* at a location near its feeder vessel–capillary junction (see panel *A*). Insets show the current traces generated before and during exposure to the pinacidil-containing perfusate. *D*, *I–V* relations recorded via a perforated-patch pipette sealed onto a pericyte located in the capillary portion (site 2) of the same

© 2009 The Authors. Journal compilation © 2009 The Physiological Society

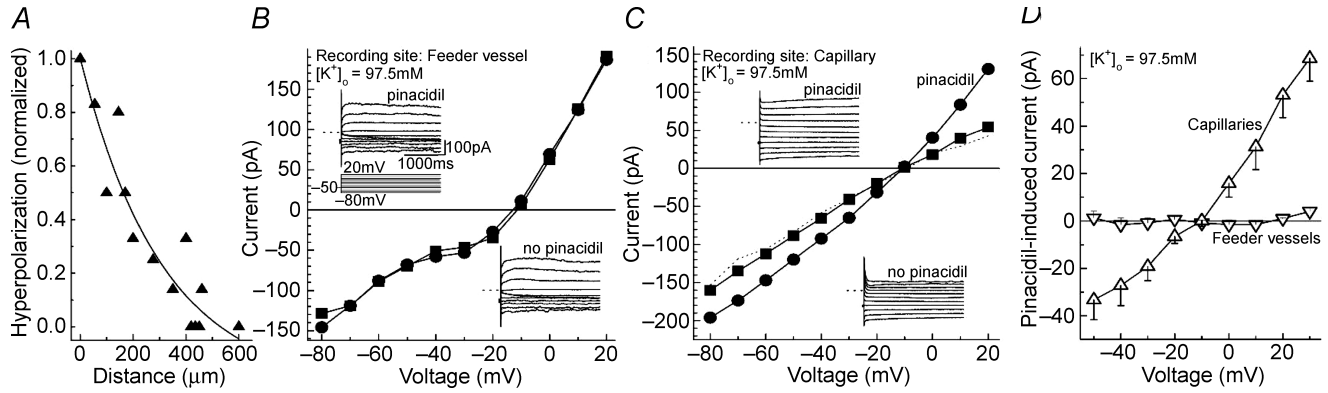

Figure 3. Use of high $[K^+]_o$ to detect pinacidil-induced currents generated in the feeder vessels and in the capillary portions of the retinal microvascular complexes

A, spread of hyperpolarization within retinal microvessels bathed in solution B (97.5 mM K^+). Solution C (3 mM K^+) was miniperfused at sites along a microvessel as a perforated-patch pipette sealed onto a mural cell monitored the voltage. For each sampled microvessel, the amplitude of the hyperpolarization generated by applying solution C at the recording site was used to normalize the voltage changes detected when solution C was applied elsewhere. Six microvessels were assessed. The line shows the fit for a first-order exponential decay. *B*, *I–V* relations recorded from the feeder vessel portion of a microvascular complex positioned in a recording chamber that was perfused with solution B without (squares) or with 5 μM pinacidil (circles). Insets show the current traces before and during pinacidil exposure, as well as the stimulus protocol used for experiments shown in panels *A–C*; dotted lines adjacent to the current traces show the zero-current level. The current and time scales apply for all current traces in this figure. A sketch of the sampled microvascular complex is presented in online Supplemental Material. *C*, *I–V* relations recorded from a pericyte located on the capillary portion of the same microvessel as studied in B. *I–V* plots were made before (squares), during (circles) and after (line without symbols) the addition of 5 μM pinacidil to solution B. Insets show the current traces used to generate the *I–V* plots. *D*, *I–V* relations of the pinacidil-induced conductance detected in feeder vessels (inverted triangles, $n = 5$) and capillaries (triangles, $n = 8$) of intact microvessels bathed in solution B.

conductance generated in the capillaries is significantly larger ($P = 0.0025$) than the conductance induced in the feeder vessels (Fig. 3*D*). Taken together, the experimental strategies of using solution B, microvessel transection and pinacidil miniperfusion yielded results that provided strong evidence that the pinacidil-induced current detected in retinal microvascular complexes is generated predominantly in the capillaries.

In other experiments, we assessed the topographical distribution of the K_{ATP} conductance induced by the vasoactive signal adenosine, whose hyperpolarizing effect on the retinal microvessels is mediated via the activation of K_{ATP} channels (Li & Puro, 2001). Using microvessels transected near their feeder vessel–capillary junction, we observed that adenosine induced a significantly greater ($P = 0.0244$) conductance in capillaries as compared with feeder vessels (Fig. 4). Taken together, our experimental results using pinacidil and adenosine support the concept that in the retinal microvasculature, there is a topographical heterogeneity

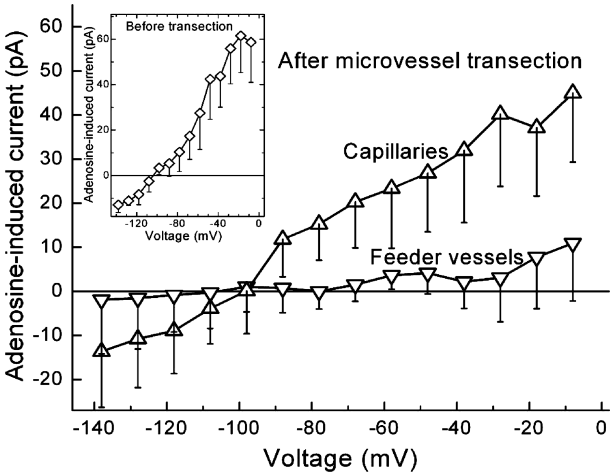

Figure 4. Adenosine-induced conductances generated in feeder vessels and capillaries

I–V relations of the current induced by the addition of 5 μM adenosine to the perfusate (solution A) in microvessels that had been transected into feeder vessel (inverted triangles, $n = 6$) and capillary (triangles, $n = 5$) portions. Inset, *I–V* plot of the adenosine-induced conductance prior to microvessel transection ($n = 6$).

transected microvessel. *E*, from a series of experiments similar to the one illustrated in panels *A–D*, the *I–V* plot of the pinacidil-induced current ($n = 11$) prior to microvessel transection. *F*, from a series of experiments similar to the one illustrated in panels *A–D*, the *I–V* relations of the pinacidil-induced current generated in capillaries (triangles, $n = 9$) and in feeder vessels (inverted triangles, $n = 7$) of *transected* microvascular complexes.

© 2009 The Authors. Journal compilation © 2009 The Physiological Society

in the distribution of functional K_{ATP} channels; most K_{ATP} current is generated in the capillaries.

Redox regulation of K_{ATP} channel function

What accounts for capillaries having a greater K_{ATP} conductance than the feeder vessels? Clearly, multiple factors could be involved. In this study, we considered the possibility that microvascular K_{ATP} channels are redox sensitive and that the redox status of capillaries enhances their K_{ATP} channel function. Although a redox sensitivity of K_{ATP} channels in the retinal microvasculature has not been reported previously, this seemed to be a reasonable possibility because K_{ATP} channels expressed in various other vascular and non-vascular tissues are redox sensitive (Islam *et al.* 1993; Inagaki *et al.* 1995; Liu & Gutterman, 2002; Avshalumov *et al.* 2005).

To help assess the redox sensitivity of K_{ATP} channels in retinal microvessels, we tested the effects of the chemical oxidant DTNB and the chemical reductant DTT. Figure 5*A* summarizes findings of a series of experiments in which the *I–V* relations of the pinacidil-induced current were determined in microvessels bathed in solution A without additives (circles), with 500 μM DTNB (triangles) or with 3 mM DTT (inverted triangles). DTNB significantly ($P = 0.0063$) increased the pinacidil-induced conductance. In contrast, DTT significantly ($P = 0.0096$) decreased this conductance. The effects of DTNB and DTT on the *I–V* relations of a retinal microvessel bathed in solution A supplemented with 5 μM pinacidil are shown in Fig. 5*B*. As illustrated in this panel, the addition of DTNB to the perfusate (solution A supplemented with 5 μM pinacidil) was associated with an increase in a hyperpolarizing current whose reversal potential was near the E_K; this observation is consistent with this oxidant activating a K^+ conductance. Subsequent exposure of this microvessel to DTT (in the continued presence of pinacidil) decreased a conductance whose reversal potential was also near E_K. Effects similar to those shown in Fig. 5*B* were observed in three other experiments. The results illustrated in Fig. 5 led us to conclude that the pinacidil-induced current in retinal microvessels is redox sensitive. Namely, oxidation increases and reduction decreases this conductance.

Even though the experiments using intact microvascular complexes bathed in solution A established that oxidation increases and reduction decreases the microvascular K_{ATP} conductance (Fig. 5), the highly efficient electrotonic transmission in microvessels assayed

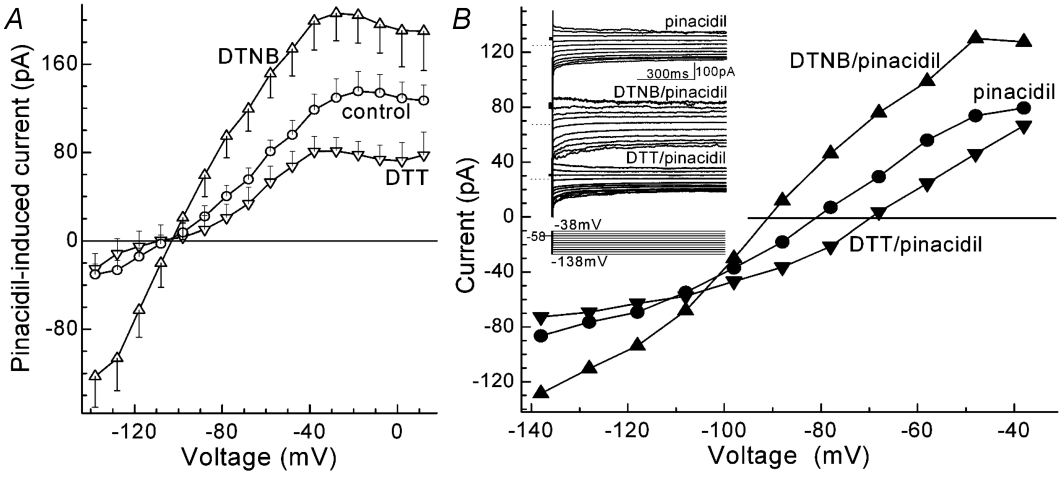

Figure 5. Effect of the oxidant DTNB and the reductant DTT
A, effects of DTNB and DTT on the pinacidil-induced conductance. *I–V* relations of the current induced by adding 5 μM pinacidil to solution A in the absence of an added oxidant or reductant (circles, $n = 16$), in the presence of 500 μM DTNB (triangles, $n = 11$), and in the presence of 3 mM DTT (inverted triangles, $n = 7$). For the DTNB group, microvessels were pre-exposed to the oxidant for 15–30 min. For the DTT group, pre-exposure to this reductant was for 12–25 min. *B*, effects of DTNB and DTT on the *I–V* relations recorded in the presence of pinacidil. Currents were monitored via a perforated-patch pipette sealed onto a mural cell located on a feeder vessel of an intact microvascular complex that had been pre-incubated for 21 min in solution A (3 mM K^+) supplemented with 5 μM pinacidil. A sketch of the sampled microvascular complex is presented in the Supplemental Material. Initially, the *I–V* relations were determined in this pinacidil-containing solution (circles). Subsequently, 500 μM DTNB was added to the solution A/pinacidil perfusate, and 26 min later *I–V* relations were again determined (triangles). DTNB was then washed out, and an *I–V* plot was generated after the microvessel was exposed for 13 min to solution A/pinacidil plus 3 mM DTT (inverted triangles). The inset shows the current traces from which the *I–V* plots were generated; the stimulus protocol is below the traces.

© 2009 The Authors. Journal compilation © 2009 The Physiological Society

in solution A (Wu *et al.* 2006) precluded determination of whether DTNB and DTT affected K_{ATP} channels located in feeder vessels and/or the capillaries. Thus, the goal of our next series of experiments was to compare the redox sensitivity of the K_{ATP} channels in the capillaries with those in the more proximal portion of the retinal microvasculature.

Figure 6*A* summarizes experiments in which microvessels transected at their feeder vessel–capillary junction were used to compare the effects of redox agents on the pinacidil-induced currents generated in feeder vessels and capillaries. In these experiments the oxidant, DTNB, increased ($P = 0.0038$) the pinacidil-induced conductance in the feeder vessels (left panel). However, in capillaries, DTNB lacked a significant ($P > 0.05$) effect (right panel). The data in Fig. 6*A* indicate that oxidation increased the feeder vessel K_{ATP} conductance so that it was not significantly different from the pinacidil-induced

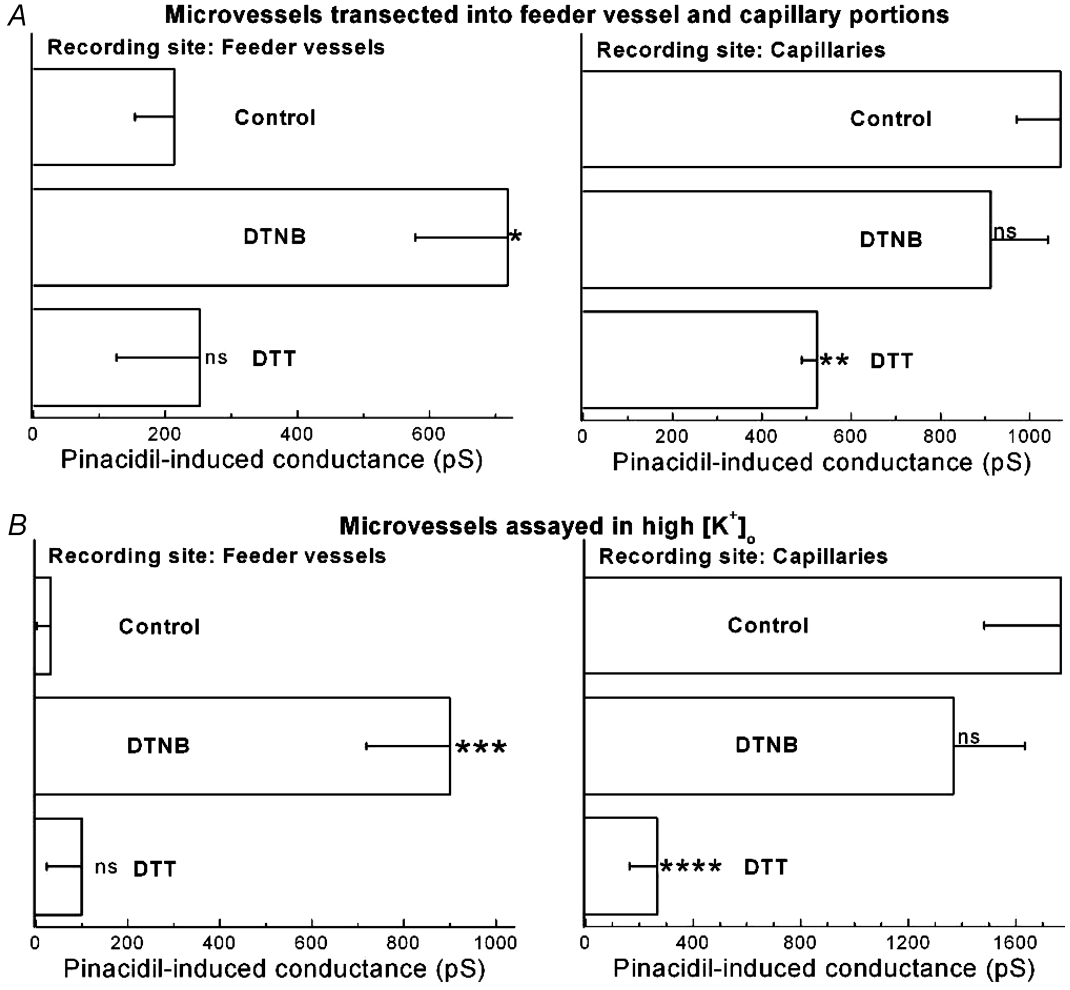

Figure 6. Effects of DTNB and DTT on the K_{ATP} conductance of feeder vessels and capillaries
A, use of microvascular complexes transected near their feeder vessel–capillary junctions to compare the effects of the oxidant DTNB and the reductant DTT on the pinacidil-induced conductances generated in feeder vessels (left panel) and capillaries (right panel). Microvessels were pre-exposed for 10–35 min to solution A supplemented with 500 μM DTNB or 3 mM DTT. The conductance induced by the subsequent addition of 5 μM pinacidil to the perfusate was then determined. The number of recordings from feeder vessels was 9 for the control, 5 for the DTNB group and 4 for the DTT group. The number of capillary recordings in the control, DTNB and DTT groups was 9, 6 and 5, respectively. $^{*}P = 0.0038$ for comparison with the feeder vessel control group; $^{**}P = 0.0268$ for comparision with the capillary control group; ns, $P > 0.05$. *B*, use of solution B (97.5 mM K^+) to compare the effects of DTNB and DTT on the pinacidil-induced conductance generated in feeder vessels (left panel) and capillaries (right panel). Microvessels were pre-exposed to 500 μM DTNB or 3 mM DTT in solution B for 10–25 min. The number of recordings from feeder vessels was 5 for the control group, 12 for the DTNB group and 7 for the DTT group. For the study of capillaries, the number of recordings for the control, DTNB and DTT groups were 8, 4 and 5, respectively. $^{***}P = 0.0006$ for comparison with the control feeder vessel group; $^{****}P = 0.0018$ for comparison with the capillary control group; ns, $P > 0.05$.

© 2009 The Authors. Journal compilation © 2009 The Physiological Society

conductance generated in capillaries under control ($P = 0.06$) or oxidizing ($P = 0.33$) conditions. In contrast to the effect of DTNB, the reductant DTT did not significantly ($P < 0.05$) affect on the pinacidil-induced conductance in the feeder vessels, but did significantly diminish ($P = 0.0268$) the pinacidil-induced conductance generated in the capillaries (right panel). In the presence of DTT, the K_{ATP} conductances of capillaries and feeder vessels were not significantly ($P = 0.11$) different.

To obtain additional evidence that exposure to a chemical oxidant increases K_{ATP} channel activity in the feeder vessels and that a chemical reductant inhibits this type of channel in the capillaries, we performed experiments with microvessels bathed in solution B, which by markedly diminishing electrotonic transmission (Fig. 3*A*) allowed detection of currents generated chiefly in the feeder vessels or in the capillaries. As shown in Fig. 6*B*, DTNB significantly increased ($P = 0.0006$) the pinacidil-induced conductance in feeder vessels (left panel), but not in the capillaries (right panel). As a result of oxidant exposure, feeder vessels and capillaries no longer had a significant ($P = 0.23$) difference in their K_{ATP} conductances.

In contrast, DTT decreased ($P = 0.0018$) the K_{ATP} current in capillaries, but not in feeder vessels. Thus, these findings are in agreement with those made in our study of transected microvessels (Fig. 6*A*).

The results of the experiments summarized in Fig. 6 led us to postulate that redox differences within a microvascular complex account, in large part, for the topographical heterogeneity in the distribution of functional K_{ATP} channels. We hypothesized that endogenous oxidants in the capillaries account for this portion of the microvasculature generating a substantial K_{ATP} conductance. Conversely, we also hypothesized that feeder vessels have a relatively reduced redox status that minimizes K_{ATP} channel function. To begin to test these hypotheses, we first wished to obtain evidence of endogenous redox activity in a retinal microvascular complex. Based on the idea that the effects of chemical reductants and oxidants are long lasting unless reversed by endogenous redox agents, we monitored *I–V* relations during the washout of DTT or DTNB. Of note, these initial experiments did not attempt to compare the redox status of feeder vessels and capillaries. Rather, we simply sought evidence for endogenous redox activity.

Figure 7*A* shows an example of an experiment in which a microvessel was initially exposed to 3 mM DTT plus 5 μM pinacidil in solution A (3 mM K^+). Subsequently, the perfusate was changed to solution A supplemented only

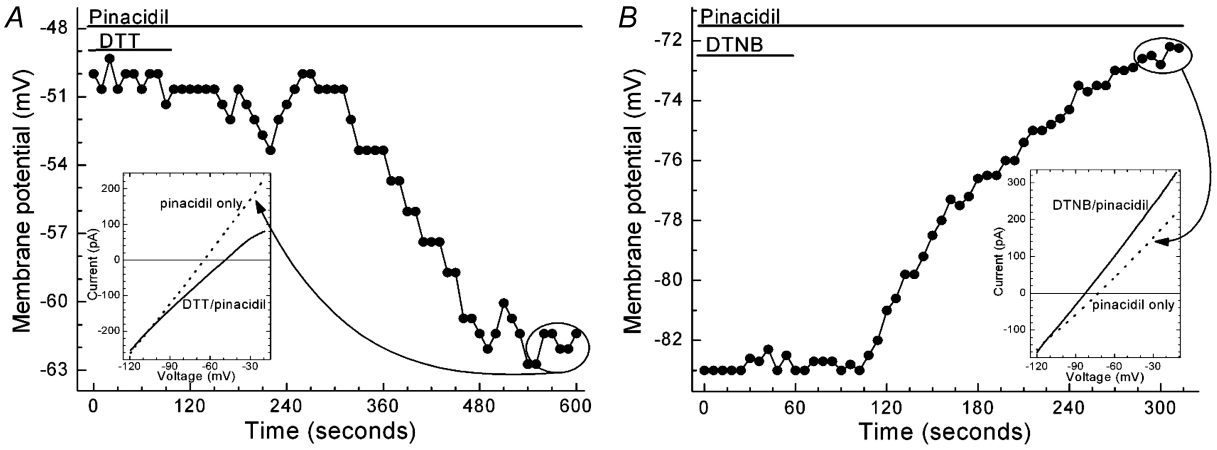

Figure 7. Membrane potential and *I–V* relations before and after washout of the chemical reductant DTT or the chemical oxidant DTNB

A, membrane potential and *I–V* relations before and after exposure to DTT. Recordings were made via a perforated-patch pipette sealed onto a mural cell located on an intact microvessel that had been exposed to solution A supplemented with 5 μM pinacidil and 3 mM DTT for 24 min prior to the onset of this recording. Bars above the data points indicate when DTT was eliminated from the perfusate. A sketch of the sampled microvascular complex is shown in the Supplemental Material. Inset shows the average of six *I–V* plots generated by a voltage-ramp protocol during the minute prior to DTT washout (continuous line) and during the final recorded minute (encircled data points) after DTT washout (dotted line). *B*, effect of DTNB washout. Prior to this recording, the microvascular complex was exposed for 20 min to solution A supplemented with 5 μM pinacidil and 500 μM DTNB. Bars indicate when DTNB was removed from in the perfusate. A sketch of the sampled microvascular complex is presented in the Supplemental Material. Inset shows the averaged *I–V* plots generated during the final minute of DTNB exposure (continuous line) and during the final 50 s (encircled data points) after DTNB washout (dotted line).

© 2009 The Authors. Journal compilation © 2009 The Physiological Society

with pinacidil (no DTT). After washout of DTT, there was a hyperpolarization caused by the activation of a current whose reversal potential was near the E_K (inset of Fig. 7*A*). In five similar experiments, the membrane potential increased ($P = 0.0308$, paired t-test) from -63 ± 5 mV in the pinacidil plus DTT solution to -71 ± 4 mV after 9.1 ± 1 min in the DTT-free perfusate.

We also tested the effect of washing out the oxidant, DTNB (Fig. 7*B*). After removal of this oxidant from the pinacidil-containing perfusate, the membrane potential decreased, as a conductance with a reversal potential near E_K diminished (inset). In a series of four similar experiments, we found that 8.4 ± 1 min after DTNB washout, the membrane potential decreased from -94 ± 1 mV to -84 ± 2 mV ($P = 0.0130$, paired t-test). From the experiments summarized in Fig. 7, we concluded that retinal microvessels have oxidant and reductant activities that modulate K_{ATP} channel function.

To determine whether there are topographical differences in the endogenous redox activity, we employed the strategy of using solution B (97.5 mM K^+), which diminishes electrotonic transmission (Fig. 3*A*). In a series of five perforated-patch recordings made from capillaries initially exposed to 5 μM pinacidil plus 3 mM DTT, we observed that 10.1 ± 1 min after washout of the chemical reductant, the conductance increased by 1270 ± 440 pS ($P = 0.0436$, paired t-test). This finding is consistent with capillaries having endogenous oxidant activity that can reverse the effect of a chemical reductant.

In other experiments, we determined the effect of DTNB washout on feeder vessels exposed to 5 μM pinacidil in solution B. In these experiments, an 11 ± 2 min washout of the chemical oxidant was associated with a 420 ± 64 pS decrease in conductance ($P = 0.019$, paired t-test; $n = 4$). This finding is consistent with feeder vessels having endogenous reductant activity that can reverse the effect of a chemical oxidant.

Of note, because DTT did not significantly affect the pinacidil-induced conductance in feeder vessels (Fig. 6), we did not assess the effect of its washout on the feeder vessel current. Likewise, because DTNB had no significant effect on the capillary conductance (Fig. 6), the effect of its washout on the pinacidil-induced conductance in capillaries was moot.

From the DTT and DTNB washout experiments, we concluded that that endogenous oxidant activity dominates in the capillaries while the redox status of feeder vessels is established by endogenous reductants. Taken together, the experiments presented in Figs 1–7 led us to conclude that redox sensitivity of microvascular K_{ATP} channels plus the dominance of endogenous oxidant activity in the capillaries accounts for these distal microvascular locations generating a substantial pinacidil-induced current. Conversely, the predominance of endogenous reductants in the feeder vessels minimizes their K_{ATP} conductance.

Spermine and the redox regulation of K_{ATP} channels

What accounts for feeder vessels and capillaries having a different redox status and thereby differing K_{ATP} channel activities? We considered the possibility that spermine is of importance. This polyamine was of interest because its catabolism is known to generate potent oxidants, such as H_2O_2 (Wang & Casero, 2006), and because an earlier study of ours suggested that the spermine concentration in the capillaries of the retinal microvasculature is higher than at more proximal microvascular sites (Matsushita & Puro, 2006). We hypothesized that the predominance of spermine-dependent oxidation in the capillaries accounts for why they generate most of the K_{ATP} current detected in a retinal microvascular complex. Conversely, we also postulated that a lower concentration of spermine in the feeder vessels allows endogenous reductants to minimize K_{ATP} channel function at these locations.

To begin to assess the role of spermine, we asked whether this polyamine increases the production of intracellular oxidants in retinal microvessels. In a series of experiments, we exposed microvessels to carboxy-H_2DCPDA, which is a cell-permeant dye that becomes fluorescent when oxidized by intracellular molecules such as H_2O_2 (Bao *et al.* 2005). As shown in Fig. 8, addition of 5 mM spermine to solution A was associated with a significant ($P < 0.0001$) increase in fluorescence intensity. We also found that the increase in fluorescence intensity during exposure of retinal microvessels to 5 mM spermine was comparable to the effect of adding 5 μM H_2O_2 to the perfusate (Fig. 8, lower inset). This concentration of extracellular H_2O_2 is thought to result in an increase in the intracellular H_2O_2 concentration that is of physiological and pathophysiological relevance, i.e. 0.5–0.7 μM (Stone, 2004). Based on these observations, we concluded that spermine-dependent oxidation can occur in retinal microvessels.

In the next series of experiments, we asked whether spermine increases the K_{ATP} conductance in retinal microvessels. The experiments summarized in Fig. 9*A* show that the addition of 5 mM spermine to solution A did increase the pinacidil-induced conductance, from 1810 ± 100 pS to 2340 ± 105 pS ($P = 0.0115$). As shown in Fig. 9*B*, the pinacidil-induced conductance generated in spermine-treated microvessels was near totally inhibited by 500 nM glibenclamide, a K_{ATP} blocker; similar results occurred in three other recordings. This effectiveness of glibenclamide is consistent with our previous study of microvascular K_{ATP} currents (Li & Puro, 2001) and supports the likelihood that pinacidil selectively activates K_{ATP} channels in the microvasculature of the

© 2009 The Authors. Journal compilation © 2009 The Physiological Society

retina. Figure 9*B* also shows that similar to our reported observation that microvessels recorded in solution A (without spermine) lack a basal K_{ATP} conductance (Li & Puro, 2001; Wu *et al.* 2001), there was no glibenclamide-sensitive current in the absence of pinacidil.

Figure 9*C* illustrates that exposure to spermine relatively rapidly resulted in the activation of a hyperpolarizing current whose reversal potential is near E_K; three other experiments showed that there was an increase in a K^+ conductance between approximately 2 and 10 min after the onset of spermine exposure. Results of the experiments illustrated in Fig. 9*A*–*C* supported the idea that spermine boosts the pinacidil-induced current in retinal microvessels.

In other experiments, we assessed the effect of an inhibitor of spermine synthesis, DL-α-difluoromethylornithine (DFMO). As shown in Fig. 9*D*, exposure of retinal microvessels to 5 mM DFMO was associated with a significant ($P = 0.0283$) decrease in the pinacidil-induced conductance. This finding indicated that endogenous spermine plays a role in modulating the function of microvascular K_{ATP} channels.

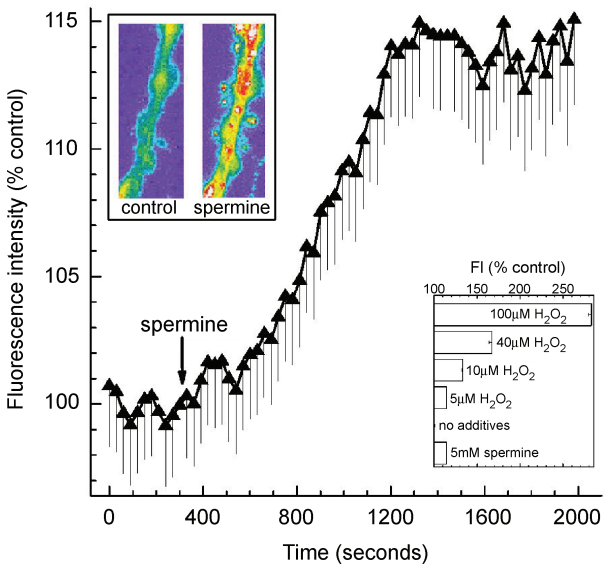

Figure 8. Effect of spermine on intracellular oxidants in retinal microvessels
Fluorescence intensity of the oxidation-sensitive dye dichlorofluorescein (DCF), before and after exposure of a retinal microvessel to 5 mM spermine. The arrow shows when spermine was added to the perfusate (solution A). Each data point is the mean of 17 regions of interest (ROIs) located in the feeder vessel portion of freshly isolated microvascular complexes. As detailed in Methods, fluorescence intensities are plotted as the percentage of the control value. Upper inset shows pseudocolour images of a portion of a monitored microvessel before (control) and 27 min after the onset of exposure to 5 mM spermine; the width of each panel in the inset is 22 μm. The lower inset shows the fluorescence intensity (FI) of DCF measured in feeder vessels 1200–1500 s after the onset of exposure to solution A with no additives ($n = 90$), with 5 mM spermine ($n = 26$) or with H_2O_2 at concentrations of 100 μM ($n = 15$), 40 μM ($n = 15$), 10 μM ($n = 15$) and 5 μM ($n = 34$). When compared to the group in which there were no additives, each experimental group had a significantly ($P < 0.0001$) greater increase in fluorescence intensity.

To help elucidate how spermine affects the function of microvascular K_{ATP} channels, we studied microvessels bathed in solution B (97.5 mM K^+), which, as noted, permits relatively independent assessments of the pinacidil-induced conductances generated in the feeder vessels and capillaries. As shown in Fig. 10, exposure of retinal microvessels to 5 mM spermine increased ($P = 0.0141$) the pinacidil-induced conductance in the feeder vessels (Fig. 10*A*), but not in the capillaries (Fig. 10*B*). Consistent with oxidation playing a role in the spermine-mediated activation of K_{ATP} channels in the feeder vessels, we observed that the chemical reductant DTT prevented this effect of spermine (Fig. 10*A*).

In other experiments to further assess the putative role of oxidation in mediating the effect of spermine on K_{ATP} channel function, we asked whether the effect of 5 mM spermine on the K_{ATP} conductance was mimicked by 5 μM H_2O_2, which has a similar effect as 5 mM spermine on the fluorescence of the oxidant-sensitive dye DCF (Fig. 8, inset). In electrophysiological experiments, we found that the pinacidil-induced conductance detected in feeder vessels exposed to solution B supplemented with 5 μM H_2O_2 was 610 ± 170 pS ($n = 6$). This is not significantly different ($P = 0.4$) from the pinacidil-induced conductance of 533 ± 135 pS generated by feeder vessels exposed to 5 mM spermine in solution B. Thus, the spermine-mediated increase in K_{ATP} current is mimicked by the oxidant H_2O_2.

In other experiments using solution B, we used the inhibitor of spermine synthesis DFMO to help assess the role of endogenous spermine in retinal capillaries. As shown in Fig. 10*B*, the pinacidil-induced conductance generated in the capillaries of DFMO-treated microvascular complexes was significantly diminished ($P = 0.0015$). This observation supports the idea that the function of K_{ATP} channels in retinal capillaries is highly dependent upon endogenous spermine.

Taken together, the experiments summarized in Figs 8–10 support our hypothesis that predominance of spermine-dependent oxidation in the capillaries accounts for why this portion of the retinal microvasculature generates most of the K_{ATP} current.

Effect of diabetes on the function of K_{ATP} channels in the retinal microvasculature

Evidence that spermine plays a role in regulating K_{ATP} channel activity in microvessels of the retina led us to postulate that pathological conditions that increase spermine in the retinal microvasculature may alter the

© 2009 The Authors. Journal compilation © 2009 The Physiological Society

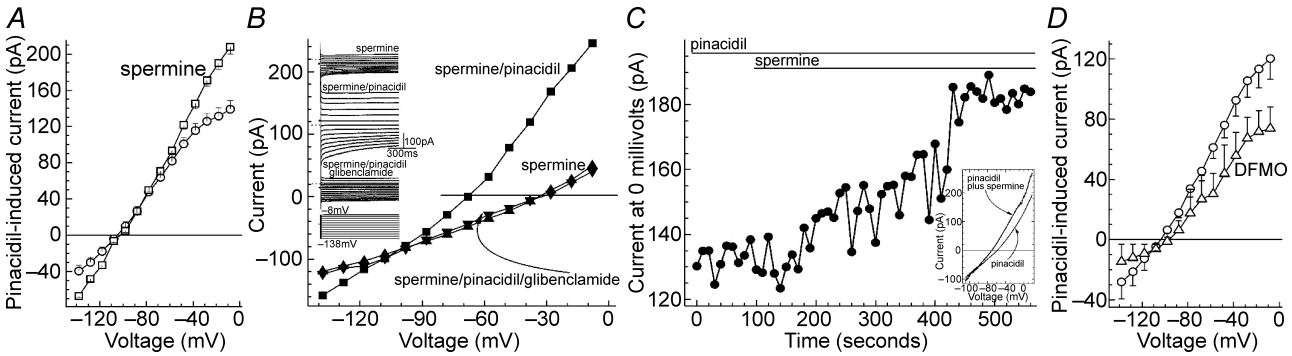

Figure 9. Spermine-mediated activation of microvascular currents
A, *I–V* plots of the pinacidil-induced conductance recorded in intact microvascular complexes exposed to perfusates containing solution A without additives (circles, $n = 34$) or with 5 mM spermine (squares, $n = 7$). In the spermine group, microvessels were pre-incubated with this polyamine for 10–30 min. Currents were recorded from mural cells on the feeder vessel portion of the microvessel. *B*, *I–V* relations generated in solution A supplemented with 5 mM spermine (triangles), with spermine and 5 μM pinacidil (squares), or with spermine plus pinacidil plus 500 nM glibenclamide (inverted triangles). The current traces used to generate the *I–V* plots are also shown. The perforated-patch recording was from an intact microvascular complex, which had been pre-exposed to solution A plus spermine for 24 min. A sketch of the sampled microvascular complex is presented in the Supplemental Material. *C*, time course for the effect of spermine on the outward current measured at 0 mV in the presence of pinacidil. Current was recorded via a perforated-patch pipette sealed onto a mural cell located on a feeder vessel portion of a microvascular complex that had been pre-incubated in solution A supplemented with 5 μM pinacidil for 11 min. The bars above the data points show when 5 mM spermine was added to this pinacidil-containing perfusate. A sketch of the sampled microvascular complex is presented in the Supplemental Material. Inset shows *I–V* plots averaged from voltage ramps run at 10 s intervals during the first and last 90 s periods. *D*, *I–V* plots of the pinacidil-induced conductance generated in microvessels that had been maintained in solution A without additives (circles, $n = 6$) for 26 ± 1 h or in solution A supplemented with 5 mM DFMO for 27 ± 1 h (triangles, $n = 5$).

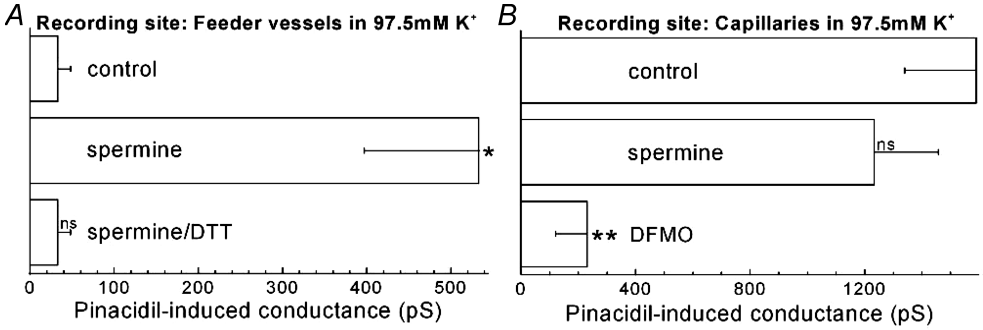

Figure 10. Use of high $[K^+]_o$ to assess the effect of spermine on the pinacidil-induced conductances generated in feeder vessels and capillaries
A, effect of spermine on the K_{ATP} conductance in feeder vessels. The K_{ATP} conductance of feeder vessels was recorded in solution B without additives (control, $n = 5$), with 5 mM spermine ($n = 6$), and with spermine plus 3 mM DTT ($n = 4$). Microvessels in the spermine group were pre-incubated for 15 to 33 min in solution B with 5 mM spermine. For the spermine/DTT group, microvessels were pre-incubated in solution B plus 3 mM DTT plus 5 mM spermine for 15 to 35 min. *$P = 0.0141$ for comparison with the control group. ns, not significantly different ($P = 1$) than control. *B*, effects of spermine and the inhibitor of spermine synthesis DFMO on the pinacidil-induced conductance recorded from the capillary portion of microvessels bathed in solution B. For the control group ($n = 13$), the effect of 5 μM pinacidil was assessed in solution B without other additives. In the spermine group ($n = 5$), microvessels were pre-exposed to this polyamine (5 mM) for 12–22 min prior to the addition of 5 μM pinacidil. For experiments using 5 mM DFMO, microvessels were exposed to this spermine synthesis inhibitor in solution A for 27 ± 1 h ($n = 6$) prior to assessing the effect of 5 μM pinacidil in solution B. Because the pinacidil-induced conductances detected in capillaries within 0.5–4 h ($n = 8$) and within 24–28 h ($n = 7$) after the isolation of retinal microvascular complexes were not significantly ($P = 0.4$) different, values from the two time periods were combined for the control group. **$P = 0.0015$ for the comparison with the control group. ns, $P = 0.25$.

© 2009 The Authors. Journal compilation © 2009 The Physiological Society

function of these channels. Because spermine is increased in the diabetic eye in general (Nicoletti *et al.* 2003) and in the feeder vessels of the retinal microvasculature in particular (Matsushita & Puro, 2006), we asked whether diabetes affects the function of K_{ATP} channels.

To begin to test the hypothesis that diabetes increases the K_{ATP} channel function in retinal microvessels, we focally applied pinacidil onto feeder vessels and capillaries of microvascular complexes isolated from rats made diabetic by streptozotocin for 7.2 ± 0.6 weeks ($n = 3$). During the miniperfusion of pinacidil, the membrane potential of a microvessel bathed in solution A was monitored via perforated-patch pipette sealed onto a mural cell. When compared with results of similar experiments using non-diabetic retinal microvessels, there was a significantly larger hyperpolarization ($P = 0.0025$) induced by the application of pinacidil onto the feeder vessel portion of diabetic microvessels (Fig. 11*A*). In contrast, the pinacidil-induced voltage change in the capillaries was not significantly ($P = 0.28$) affected by diabetes (Fig. 11*B*). These findings demonstrated that diabetes increases the K_{ATP}-induced hyperpolarization generated in the feeder vessels of the retinal microvasculature.

In a series of voltage-clamp recordings, we measured the pinacidil-induced conductances in the feeder vessel and capillary portions of non-diabetic and diabetic microvessels that had been transected near their feeder vessel–capillary junctions. As shown in Fig. 11*C*, diabetes significantly ($P = 0.0105$) increased the pinacidil-induced conductance generated in the feeder vessels. In contrast, the conductance induced in capillaries by pinacidil was not significantly ($P = 0.35$) affected by diabetes (Fig. 11*D*). Thus, similar to the experiments in which we focally applied pinacidil, the results of experiments using

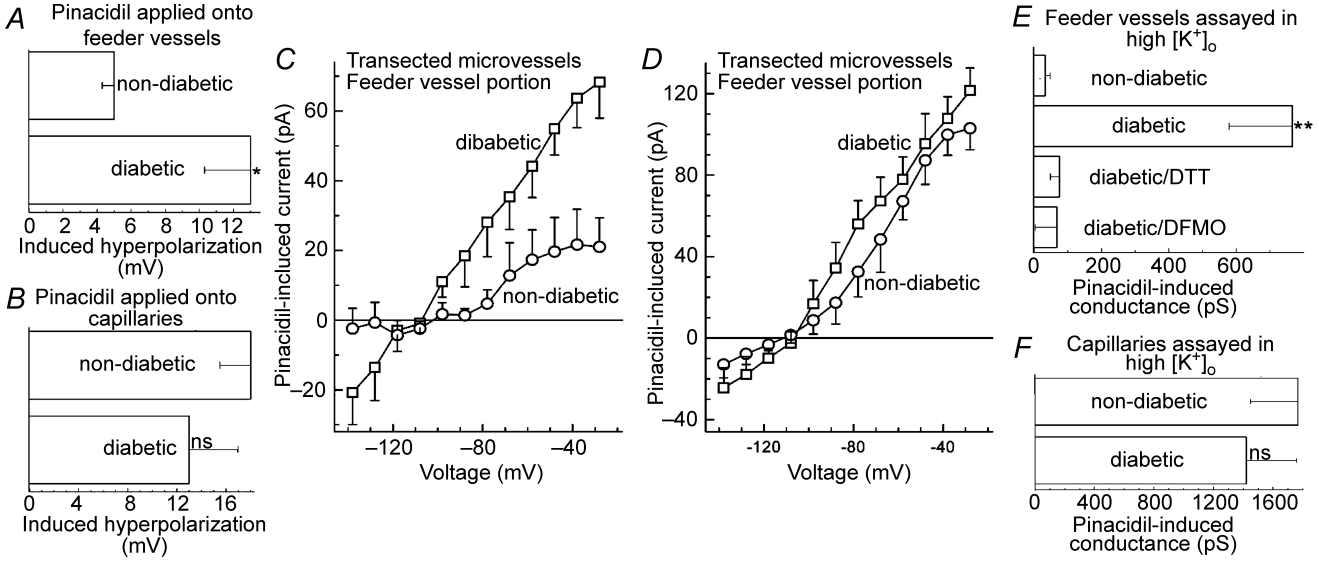

Figure 11. Effect of diabetes on K_{ATP} channel function in feeder vessels and capillaries
A, comparison in solution A (3 mM K^+) of the hyperpolarizing effects of focally applying pinacidil onto the feeder vessel portion of non-diabetic ($n = 29$) and diabetic ($n = 9$) retinal microvessels. $^*P = 0.0025$. *B*, similar to *A*, but with pinacidil focally applied onto capillaries. For the non-diabetic and the diabetic groups, 19 and 9 microvessels were assessed, respectively. ns, not significant ($P = 0.28$). *C*, *I–V* plots of the pinacidil-induced conductances in the feeder vessel portion of non-diabetic ($n = 7$) and diabetic ($n = 15$) microvascular complexes that had been transected near their feeder vessel–capillary junctions. Solution A without and with 5 μM pinacidil was used in these experiments. *D*, in transected microvessels, the pinacidil-induced currents recorded in capillaries of non-diabetic ($n = 9$) and diabetic ($n = 4$) microvascular complexes. Solution A without and with 5 μM pinacidil was used in these experiments. *E*, use of solution B (97.5 mM K^+) to quantify the pinacidil-induced conductance detected in recordings from feeder vessels of non-diabetic and diabetic microvessels. For the non-diabetic and diabetic groups, 5 and 15 microvessels were assessed, respectively. In the diabetic/DTT group ($n = 6$), microvessels were pre-exposed to 3 mM DTT in solution B for 10–25 min prior to the generation of *I–V* relations without and with the addition of 5 μM pinacidil to DTT-containing solution. For the diabetic/DFMO group ($n = 5$), microvessels were exposed to 5 mM DFMO in solution A for 23–26 h prior to assaying the pinacidil-induced conductance in solution B. Because the pinacidil-induced conductances detected in diabetic microvessels 0.5–4 h ($n = 8$) and 23–26 h ($n = 7$) after isolation from the retina were not significantly different ($P = 0.5$), values from these time periods were combined for the diabetic group that was not exposed to either DTT or DFMO. $^{**}P = 0.0059$ for comparison with the non-diabetic group. In diabetic retinal microvessels, DTT and DFMO significantly ($P \leq 0.0051$) decreased the pinacidil-induced conductance. *F*, pinacidil-induced conductances in the capillary portion of non-diabetic ($n = 8$) and diabetic ($n = 5$) microvessels bathed in solution B. ns, not significantly different ($P = 0.14$).

© 2009 The Authors. Journal compilation © 2009 The Physiological Society

transected microvessels were consistent with diabetes increasing K_{ATP} channel activity in the feeder vessels, but not in the capillaries.

Based on our finding that there is an increase in K_{ATP} channel function in the microvasculature of the diabetic retina (Fig. 11*C* and *D*), we wished to assess the effect of adenosine, which is a vasoactive signal that activates these channels (Li & Puro, 2001; Wu *et al.* 2001). We predicted that adenosine should evoke a larger hyperpolarization in diabetic, as compared with non-diabetic, microvessels. In agreement with this, we found that 5 μM adenosine induced a 38 ± 3.6 mV ($n = 11$) hyperpolarization in diabetic retinal microvessels, while non-diabetic vessels were hyperpolarized by 28 ± 1.7 mV ($P = 0.0062$, $n = 24$). Thus, the diabetes-induced increase in functional K_{ATP} channels boosts the hyperpolarizing response of the retinal microvasculature to adenosine.

Additional studies (Fig. 11*E* and *F*) employed the strategy of assaying the pinacidil-induced conductance in microvascular complexes bathed in solution B (97.5 mM K^+). As with experiments using transected microvessels (Fig. 11*C* and *D*), we observed that the pinacidil-induced conductance generated in feeder vessels was markedly ($P = 0.0059$) greater in diabetic, as compared with non-diabetic, microvessels (Fig. 11*E*). Also in agreement with experiments using transected microvessels, diabetes did not significantly ($P = 0.14$) affect the K_{ATP} current in the capillaries (Fig. 11*F*). Consistent with oxidation playing an important role in mediating the diabetes-induced increase in the K_{ATP} current generated in feeder vessels, this effect was reversed by exposing diabetic microvessels to the chemical reductant DTT (Fig. 11*F*). We also documented that the diabetes-induced increase in the K_{ATP} current generated in feeder vessels was reversed by exposure of diabetic microvessels to the inhibitor of spermine synthesis DFMO (Fig. 11*E*). This effect of DFMO is consistent with intracellular spermine playing a critical role in the mechanism by which diabetes increases K_{ATP} channel function in feeder vessels of the retinal microvasculature. Taken together, the results summarized in Fig. 11 support the scenario that in microvascular complexes of the diabetic retina, a mechanism involving spermine-dependent oxidation accounts for the observed increase in the K_{ATP} current generated in the feeder vessels.

Discussion

Based on experiments using microvascular complexes freshly isolated from the rat retina, this study provides new insights into mechanisms regulating the function of K_{ATP} channels in the retinal microvasculature. Our experiments demonstrated that these ion channels, which mediate the hyperpolarizing effects of vasoactive signals such as adenosine and dopamine (Li & Puro, 2001; Wu *et al.* 2001), are potently regulated by redox conditions. A key conclusion of this study is that the oxidation-mediated modulation of microvascular K_{ATP} channels is driven by the polyamine spermine, whose catabolism is known to generate H_2O_2 and other oxidants (Wang & Casero, 2006). In support of spermine-dependent oxidation playing a modulatory role, we documented that exposure of microvessels to this polyamine not only increased intracellular oxidants, but also increased the K_{ATP} current by a reductant-sensitive mechanism. Further support for the idea that endogenous spermine is linked with the functioning of microvascular K_{ATP} channels was our finding that inhibition of the synthesis of spermine in retinal microvessels results in a marked decrease in current induced by the K_{ATP} activator pinacidil. Taken together, our experiments indicate that spermine-dependent oxidation is a previously unrecognized mechanism by which ion channel function can be modulated by this polyamine, whose direct binding to membrane-bound molecules is well-known to affect a variety of channels (Lopatin *et al.* 1994; Fearon *et al.* 1999; Mortensen *et al.* 1999; Nilsson *et al.* 2002). In the retinal microvasculature, it appears that spermine-dependent oxidation plays a critically important role in the regulation of K_{ATP} channels.

Another key conclusion of our study is that the K_{ATP} current detected in retinal microvascular complexes is predominately generated in the capillaries. Our experiments indicate that the topographical distribution of functional K_{ATP} channels in the retinal microvasculature is due, in large part, to the predominance of spermine-dependent oxidation in the capillaries. Conversely, at more proximal sites in the retinal microvasculature, the redox status is dominated by endogenous reductants, and the function of redox-sensitive K_{ATP} channels is minimized. This study appears to be the first to demonstrate that the redox status can vary markedly across a microvascular complex. Also, an additional new finding is that regional differences in redox status can play a significant role in determining the functional organization of a feeder vessel–capillary unit.

Our observation that there is a substantial difference in the magnitude of the K_{ATP} conductance generated by retinal capillaries, as compared with their feeder vessels, strongly suggests that these contiguous regions of a microvascular complex are physiologically specialized even though together they constitute a highly interactive functional unit (Wu *et al.* 2006). By possessing most of the functional K_{ATP} channels, capillaries appear to be specialized for transducing the activation of receptors for adenosine and dopamine into a voltage change, which subsequently mediates a vasomotor response. We postulate that the initiation of voltage responses at decentralized sites enhances the spatial resolution of extracellular

© 2009 The Authors. Journal compilation © 2009 The Physiological Society

vasoactive inputs and thereby tightens the coupling of capillary perfusion to local metabolic demand. The initiation of a K_{ATP}-induced vascular response predominately in the capillaries supports the organizational concept that decentralized components of the microvasculature are physiologically adapted to play an important role in the regulation of local perfusion in the retina.

What are the functional consequences of a K_{ATP}-mediated hyperpolarization generated within the retinal microvasculature? Although the adenosine-induced activation of K_{ATP} channels in large retinal arterioles ($> 90\ \mu$m diameter) is known to cause these vessels to dilate and blood flow to increase (Gidday *et al.* 1996), little has been reported about the functional effects of K_{ATP} channel activation in the distal portion of the retina's circulatory system. However, in unpublished experiments on freshly isolated retinal microvascular complexes consisting of small arterioles ($< 20\ \mu$m diameter), feeder vessels and capillaries, we have observed that pinacidil and adenosine cause mural cells on feeder vessels and arterioles to relax and lumens of these microvessels to dilate (M. Kobayashi, K. Katsumura, M. Minami & D. Puro, unpublished observations). In contrast, we have not detected pinacidil- or adenosine-induced relaxation of pericytes located on the abluminal wall of retinal capillaries (M. Kobayashi, K. Katsumura, M. Minami & D. Puro, unpublished observations).

What accounts for the lack of pericyte relaxation during a K_{ATP}-mediated hyperpolarization? The absence of relaxation is not due to an inability of pericytes to change their contractile tone. In fact, numerous vasoactive signals elicit robust contractile responses in pericytes located on freshly isolated microvascular complexes (Puro, 2007), as well as in the intact retina (Peppiatt *et al.* 2006). Rather, our unpublished studies indicate that retinal pericytes do not relax during hyperpolarization because voltage-dependent calcium channels (VDCCs) have a minimal role in establishing the basal calcium concentration of these mural cells (T. Kobayashi & D. Puro, unpublished observations). As a consequence, hyperpolarization does not significantly decrease pericyte calcium (T. Kobayashi & D. Puro, unpublished observations). In contrast, mural cells at proximal microvascular sites have significant basal activity of their VDCCs, whose inactivation by hyperpolarization results in a decrease in intracellular calcium and thereby relaxation (T. Kobayashi & D. Puro, unpublished observations). From these observations, we hypothesize that the low level of basal VDCC activity in retinal pericytes requires that a K_{ATP}-mediated hyperpolarization must be transmitted electrotonically to proximal microvascular locations where the increase in membrane potential diminishes VDCC activity, reduces intracellular calcium and thereby results in mural cell relaxation and vasodilatation. On the other hand, we also posit that when depolarization by vasoactive signals, such as endothelin-1, angiotensin II and ATP (Peppiatt *et al.* 2006; Puro, 2007), activates pericyte VDCCs, a subsequent K_{ATP}-mediated hyperpolarization could close VDCCs, lessen intracellular calcium and cause pericytes to relax and capillaries to dilate. In this way, vasomotor activity in retinal capillaries may play an active role in effecting a change in blood flow when K_{ATP} channels are activated by extracellular molecules, such as adenosine and dopamine. However, it is clear that further experimental work will be necessary to more fully clarify the functional dynamics of the capillary–feeder vessel unit within the retinal microvasculature.

Because dysregulation of retinal blood flow occurs early in the course of diabetes (Kohner *et al.* 1995) and may play a role in the progression of diabetic retinopathy, this study considered the possibility that K_{ATP} channel function in the microvascular may be altered by this pathological condition. In this study, we observed that soon after the onset of streptozotocin-induced diabetes, K_{ATP} channel activity in the retinal microvasculature increased markedly in the vessels located just proximal to a capillary network, i.e. the feeder vessels. Consistent with spermine-dependent oxidation mediating this up-regulation, the diabetes-induced increase in K_{ATP} current was reversed when microvessels were exposed to the inhibitor of spermine synthesis DFMO or the chemical reductant DTT. Also consistent with a role for spermine, we previously reported that a short duration of streptozotocin-induced hyperglycaemia appears to increase spermine in the proximal microvasculature of the retina (Matsushita & Puro, 2006). Furthermore, the demonstration presented here that exposure of non-diabetic microvessels to spermine mimics the effect of diabetes on the proximally generated K_{ATP} current provides additional support for this polyamine mediating the diabetes-induced increase in K_{ATP} conductance. Thus, in addition to identifying spermine-dependent oxidation as an important physiological mechanism regulating the activity of microvascular K_{ATP} channels, this study also raises the possibility that spermine-dependent oxidation contributes to diabetes-induced changes in the function of the retinal microvasculature.

What are the consequences of the diabetes-induced increase in K_{ATP} current at proximal microvascular sites? One consequence is the near total abolition of the topographical heterogeneity in the distribution of functional K_{ATP} channels within the retinal microvasculature. With this diabetes-induced alteration in the functional organization of the retinal microvasculature, K_{ATP}-mediated hyperpolarizations are no longer generated almost exclusively at decentralized sites. A hypothesis awaiting testing is that less decentralization of blood flow control in the diabetic retina adversely affects

© 2009 The Authors. Journal compilation © 2009 The Physiological Society

the efficacy by which capillary perfusion is matched to local metabolic needs.

Although a diabetes-induced increase in spermine-dependent oxidants is likely to have adverse effects on the function of the retinal microvasculature, there may be potentially beneficial consequences. For example, when a vasoactive signal, such as adenosine, is released at sites throughout the retinal microvascular tree, the diabetes-induced increase in K_{ATP} conductance provides a boost in the induced hyperpolarization. This boost, which is documented in this study, is likely to enhance the vasorelaxing response to adenosine, whose extracellular concentration in the retina is increased by hypoxia and ischaemia (Roth *et al.* 1997). In this way, blood flow to regions of metabolic compromise may be facilitated in the diabetic retina.

Another potential benefit of a diabetes-induced increase in K_{ATP} channel activity is suggested by our earlier study of metabolically compromised retinal microvessels (Kodama *et al.* 2001). In that study, we observed that cell death was significantly decreased when K_{ATP} channel activity was boosted. Thus, an up-regulation of K_{ATP} channel function in the diabetic retina may be vasoprotective. Perhaps a tipping point for the progression of diabetic retinopathy occurs when the beneficial effects of increased K_{ATP} channel activity are counterbalanced by the adverse consequences of lessening the decentralized control of capillary perfusion.

Our conclusion that the redox status of the retinal capillaries is driven by spermine-dependent oxidation raises the possibility of an additional pathophysiological scenario. We hypothesize that the chronic presence of oxidants generated from the catabolism of spermine makes cells of the capillaries particularly vulnerable to the increased oxidant production that occurs with diabetes (Brownlee, 2001). The possibility that capillaries of the retina are normally on the brink of a toxic overload of oxidants is intriguing because capillary cell death is one of the earliest events in diabetic retinopathy (Cogan *et al.* 1961; Mizutani *et al.* 1996). Future experimental studies will assess the possibility that spermine-dependent oxidation accounts, at least in part, for the susceptibility of retinal capillaries to diabetes-induced damage.

The conclusions of this study are based on experiments performed on microvascular complexes freshly isolated from the rat retina. An advantage of studying isolated microvascular complexes is that the vascular effects of chemicals, such as spermine, pinacidil, adenosine, DTNB, DTT and DFMO, can be assessed in the absence of confounding effects mediated via non-vascular cells. In addition, isolated microvessels greatly facilitate the ability to focally apply pharmacological agents onto specific regions of the retinal microvasculature. Also, our preparation allows pericytes of capillaries and mural cells of feeder vessels to be unambiguously indentified by an experimenter and efficiently sealed onto with patch pipettes. On the other hand, our glia- and neuron-free preparation is of limited use for directly assessing how neuronal activity alters blood flow or how a rise in glial cell calcium elicits vasomotor responses, as observed in the intact retina (Metea & Newman, 2006). An addition caveat is that our isolated microvessels were not internally perfused, and thus, the effects of blood flow on ion channel function were not addressed. Another caution is that confirmation of the conclusions derived from our study of isolated microvascular complexes awaits technical advances that will permit experiments comparable to those presented here to be performed on retinal microvessels *in vivo*. Future studies are also needed to elucidate the molecular details of the redox regulation of K_{ATP} channel function. Furthermore, because spermine is reported to modulate cardiac K_{ATP} channel activity by binding to the channel or to neighbouring membrane sites (Niu & Meech, 1998), there is a need to assess whether this polyamine regulates the function of microvessel K_{ATP} channels by a mechanism in addition to spermine-dependent oxidation. Finally, we note that one should be cautious in extrapolating our findings to other vascular beds because capillaries in some tissues appear not to express K_{ATP} channels (Bondjers *et al.* 2006) and also because the retina's circulatory system has special adaptations to meet the unique challenge of vascularizing a translucent tissue. However, despite caveats, our experimental approach has revealed previously unappreciated physiological and pathophysiological concepts concerning the retinal microvasculature.

In summary, we conclude that the function of K_{ATP} channels in microvessels of the retina is potently regulated by a redox mechanism driven by the polyamine spermine, whose catabolism is known to produce oxidants. Our experiments revealed that the predominance of spermine-dependent oxidation in the capillary network accounts for why the K_{ATP} current detected in a retinal microvascular complex is generated predominately in the capillaries. In addition to identifying spermine-dependent oxidation as a physiological mechanism modulating microvascular K_{ATP} channels, our results also support the possibility that a diabetes-induced increase in spermine-dependent oxidation alters the functional organization and perhaps the functional capabilities of the retinal microvasculature.

References

Avshalumov MV, Chen BT, Koos T, Tepper JM & Rice ME (2005). Endogenous hydrogen peroxide regulates the excitability of midbrain dopamine neurons via ATP-sensitive potassium channels. *J Neurosci* **25**, 4222–4231.

© 2009 The Authors. Journal compilation © 2009 The Physiological Society

Bao L, Avshalumov MV & Rice ME (2005). Partial mitochondrial inhibition causes striatal dopamine release suppression and medium spiny neuron depolarization via H_2O_2 elevation, not ATP depletion. *J Neurosci* **25**, 10029–10040.

Barry PH (1994). JPCalc, a software package for calculating liquid junction potential corrections in patch-clamp, intracellular, epithelial and bilayer measurements and for correcting junction potential measurements. *J Neurosci Methods* **51**, 107–116.

Bondjers C, He L, Takemoto M, Norlin J, Asker N, Hellstrom M, Lindahl P & Betsholtz C (2006). Microarray analysis of blood microvessels from PDGF-B and PDGF-Rβ mutant mice identifies novel markers for brain pericytes. *FASEB J* **20**, 1703–1705.

Brownlee M (2001). Biochemistry and molecular cell biology of diabetic complications. *Nature* **414**, 813–820.

Buttery RG, Hinrichsen CF, Weller WL & Haight JR (1991). How thick should a retina be? A comparative study of mammalian species with and without intraretinal vasculature. *Vision Res* **31**, 169–187.

Chase J (1982). The evolution of retinal vascularization in mammals. A comparison of vascular and avascular retinae. *Ophthalmology* **89**, 1518–1525.

Cogan DG, Toussaint D & Kuwabara T (1961). Retinal vascular patterns. IV. Diabetic retinopathy. *Arch Ophthalmol* **166**, 366–378.

Fearon IM, Palmer AC, Balmforth AJ, Ball SG, Varadi G & Peers C (1999). Modulation of recombinant human cardiac L-type Ca^{2+} channel α1C subunits by redox agents and hypoxia. *J Physiol* **514**, 629–637.

Funk RH (1997). Blood supply of the retina. *Ophthalmic Res* **29**, 320–325.

Gidday JM, Maceren RG, Shah AR, Meier JA & Zhu Y (1996). K_{ATP} channels mediate adenosine-induced hyperemia in retina. *Invest Ophthalmol Vis Sci* **37**, 2624–2633.

Ikebe T, Shimada T, Ina K, Kitamura H & Nakatsuka K (2001). The three-dimensional architechture of retinal blood vessels in KK mice, with special reference to the smooth muscle cells and pericytes. *J Electron Microsc (Tokyo)* **50**, 125–133.

Inagaki N, Gonoi T, Clement JP 4th, Namba N, Inazawa J, Gonzalez G, Aguilar-Bryan L, Seino S & Bryan J (1995). Reconstitution of I_{KATP}: an inward rectifier subunit plus the sulfonylurea receptor. *Science* **270**, 1166–1170.

Islam MS, Berggren PO & Larsson O (1993). Sulfhydryl oxidation induces rapid and reversible closure of the ATP-regulated K^+ channel in the pancreatic β-cell. *FEBS Lett* **319**, 128–132.

Kawamura H, Oku H, Li Q, Sakagami K & Puro DG (2002). Endothelin-induced changes in the physiology of retinal pericytes. *Invest Ophthalmol Vis Sci* **43**, 882–888.

Kawamura H, Kobayashi M, Li Q, Yamanishi S, Katsumura K, Minami M, Wu DM & Puro DG (2004). Effects of angiotensin II on the pericyte-containing microvasculature of the rat retina. *J Physiol* **561**, 671–683.

Kawamura H, Sugiyama T, Wu DM, Kobayashi M, Yamanishi S, Katsumura K & Puro DG (2003). ATP: a vasoactive signal in the pericyte-containing microvasculature of the rat retina. *J Physiol* **551**, 787–799.

Kobayashi T & Puro DG (2007). Loss of insulin-mediated vasoprotection: early effect of diabetes on pericyte-containing microvessels of the retina. *Invest Ophthalmol Vis Sci* **48**, 2350–2355.

Kodama T, Oku H, Kawamura H, Sakagami K & Puro DG (2001). Platelet-derived growth factor-BB: a survival factor for the retinal microvasculature during periods of metabolic compromise. *Curr Eye Res* **23**, 93–97.

Kohner EM, Patel V & Rassam SM (1995). Role of blood flow and impaired autoregulation in the pathogenesis of diabetic retinopathy. *Diabetes* **44**, 603–607.

Li Q & Puro DG (2001). Adenosine activates ATP-sensitive K^+ currents in pericytes of rat retinal microvessels: role of A_1 and A_{2a} receptors. *Brain Res* **907**, 93–99.

Liu Y & Gutterman DD (2002). Oxidative stress and potassium channel function. *Clin Exp Pharmacol Physiol* **29**, 305–311.

Lopatin AN, Makhina EN & Nichols CG (1994). Potassium channel block by cytoplasmic polyamines as the mechanism of intrinsic rectification. *Nature* **372**, 366–369.

Matsushita K & Puro DG (2006). Topographical heterogeneity of K_{IR} currents in pericyte-containing microvessels of the rat retina: effect of diabetes. *J Physiol* **573**, 483–495.

Metea MR & Newman EA (2006). Glial cells dilate and constrict blood vessels: a mechanism of neurovascular coupling. *J Neurosci* **26**, 2862–2870.

Mizutani M, Kern TS & Lorenzi M (1996). Accelerated death of retinal microvascular cells in human and experimental diabetic retinopathy. *J Clin Invest* **97**, 2883–2890.

Mortensen M, Matsumoto I, Niwa S & Dodd PR (1999). The modulatory effect of spermine on the glutamate-NMDA receptor is regionally variable in normal human adult cerebral cortex. *Pharmacol Toxicol* **84**, 135–142.

Nicoletti R, Venza I, Ceci G, Visalli M, Teti D & Reibaldi A (2003). Vitreous polyamines spermidine, putrescine, and spermine in human proliferative disorders of the retina. *Br J Ophthalmol* **87**, 1038–1042.

Nilsson BO, Gomez MF, Sward K & Hellstrand P (2002). Regulation of Ca^{2+} channel and phosphatase activities by polyamines in intestinal and vascular smooth muscle: implications for cellular growth and contractility. *Acta Physiol Scand* **176**, 33–41.

Niu XW & Meech RW (1998). The effect of polyamines on K_{ATP} channels in guinea-pig ventricular myocytes. *J Physiol* **508**, 401–411.

Oku H, Kodama T, Sakagami K & Puro DG (2001). Diabetes-induced disruption of gap junction pathways within the retinal microvasculature. *Invest Ophthalmol Vis Sci* **42**, 1915–1920.

Peppiatt CM, Howarth C, Mobbs P & Attwell D (2006). Bidirectional control of CNS capillary diameter by pericytes. *Nature* **443**, 700–704.

Puro DG (2007). Physiology and pathobiology of the pericyte-containing retinal microvasculature: new developments. *Microcirculation* **14**, 1–10.

Roth S, Rosenbaum PS, Osinski J, Park SS, Toledano AY, Li B & Moshfeghi AA (1997). Ischemia induces significant changes in purine nucleoside concentration in the retina-choroid in rats. *Exp Eye Res* **65**, 771–779.

Shepro D & Morel NM (1993). Pericyte physiology. *FASEB J* **7**, 1031–1038.

© 2009 The Authors. Journal compilation © 2009 The Physiological Society

Stone JR (2004). An assessment of proposed mechanisms for sensing hydrogen peroxide in mammalian systems. *Arch Biochem Biophys* **422**, 119–124.

Wang Y & Casero RA Jr (2006). Mammalian polyamine catabolism: a therapeutic target, a pathological problem, or both? *J Biochem* **139**, 17–25.

Wu DM, Kawamura H, Li Q & Puro DG (2001). Dopamine activates ATP-sensitive K^+ currents in rat retinal pericytes. *Vis Neurosci* **18**, 935–940.

Wu DM, Kawamura H, Sakagami K, Kobayashi M & Puro DG (2003). Cholinergic regulation of pericyte-containing retinal microvessels. *Am J Physiol Heart Circ Physiol* **284**, H2083–H2090.

Wu DM, Miniami M, Kawamura H & Puro DG (2006). Electrotonic transmission within pericyte-containing retinal microvessels. *Microcirculation* **13**, 353–363.

Yamanishi S, Katsumura K, Kobayashi T & Puro DG (2006). Extracellular lactate as a dynamic vasoactive signal in the rat retinal microvasculature. *Am J Physiol Heart Circ Physiol* **290**, H925–H934.

Ye XD, Laties AM & Stone RA (1990). Peptidergic innervation of the retinal vasculature and optic nerve head. *Invest Ophthalmol Vis Sci* **31**, 1731–1737.

Zhao HB & Santos-Sacchi J (1998). Effect of membrane tension on gap junctional conductance of supporting cells in Corti's organ. *J Gen Physiol* **112**, 447–455.

Author contributions

All experiments were performed at the University of Michigan by E.I. and M.F; they also contributed to the design of experiments, the analysis of data and the critical review of drafts of the manuscript. D.G.P. led in the conception and design of the project, in the analysis of the data, and in the writing of the manuscript. All authors gave final approval of the version to be published.

Acknowledgements

The authors thank Bret Hughes and David M. Wu for helpful discussions. This work was supported by grants from the National Institutes of Health, EY12505 and EY07003. D.G.P. is a Research to Prevent Blindness Senior Scientific Scholar.

Supplemental material

Online supplemental material for this paper can be accessed at: http://jp.physoc.org/cgi/content/full/jphysiol.2009.169003/DC1

© 2009 The Authors. Journal compilation © 2009 The Physiological Society